FINITE ELEMENT ANALYSIS FOR HYSTERETIC BEHAVIOR OF THIN-WALLED STEEL BRIDGE PIERS WITH PARTIALLY IN-FILLED CONCRETE

コンクリート部分充填鋼製橋脚の履歴挙動の有限要素解析

A Dissertation Submitted in Partial Fulfillment of the Requirements for the Degree of Doctor of Engineering.

Ghosh Prosenjit Kumar

ゴーシュ ポロセンジト クマール

Supervised by

Professor Yoshiaki Goto

後藤 芳顯教授

Department of Civil Engineering, Nagoya Institute of Technology
Gokiso-cho, Showa-ku, Nagoya 466, Japan

名古屋工業大学 社会開発工学専攻

January, 2009

名古屋工業大学博士論文
甲第700号(課程修了による)
平成21年3月23日授与

ABSTRACT

Partially concrete filled thin-walled steel tubular (PCFT) columns are often used for elevated highway bridge piers in Japan due to the high earthquake resistance. This is because the local buckling of steel tubes is restrained by the in-filled concrete that is confined by diaphragms and their strength and ductility are considerably improved. As observed in 1995 Kobe earthquake, the damages of the columns are usually influenced by the in-put earthquake waves and Japanese seismic design code for highway bridges adopted a new design concept to control the damage of the columns. Therefore, the control of the local buckling under cyclic loading is very important to improve the energy dissipation capacity as well as to prevent the overall failure of PCFT columns. The cyclic local buckling that usually governs the ultimate behavior of thin-walled steel columns is prevented by the complicated interface action between steel & concrete and internal passive pressure due to dilation of in-filled concrete. On the other hand, this pressure that acts as confinement to the in-filled concrete also increases the strength of concrete. Therefore, an accurate modeling of the interface action together with the behavior of confined concrete and thin-walled steel tube may be an only versatile method to predict the hysteretic behavior of PCFT columns in a direct manner. However, up to the present, no research has been conducted on the analysis of PCFT column in a direct manner due to the difficulty of the modeling that assures numerical stability. To construct the FEM model, the steel tube and in-filled concrete are modeled with geometrically and materially nonlinear shell elements and solid elements, respectively. To ensure the interface action between steel and concrete, contact and friction behaviors are considered. To express the material constitutive relation, the 3-surface cyclic plasticity model is used for the steel tube, while the concrete damaged plasticity model is used for the in-filled concrete. Herein, first, an accurate and numerically stable FEM model is proposed to compute the hysteretic behavior of PCFT columns and then, accuracy of the computed results is confirmed by comparing with experimental results. Furthermore, based on proposed FEM model, the mechanical properties of PCFT columns are investigated with considering occurrence of fracture in steel tube, in-filled concrete restraining effect on strength, ductility and energy dissipation capacity as well as confining pressure effect on concrete strength.

TABLE OF CONTENTS

LIST OF FIGURES

LIST OF TABLES

PREFACE

In this research an accurate and stable FEM model is proposed to compute the hysteretic behavior of thin-walled steel bridge piers with partially in-filled concrete. The thesis consists of four chapters. The contents of each chapter are briefly described.

Chapter 1 (Introduction): This chapter includes general introduction, background and objective of the present research. In 1995, elevated highway bridge piers in Japan were seriously damaged due to Kobe earthquake. To control the damages of the columns, it is necessary to restrain the cyclic local buckling of steel tube. Thin-walled steel tubular columns with partially in-filled concrete (PCFT) will be an alternative approach to control the damages of the columns. To investigate the hysteretic behavior of PCFT columns, there are several experimental studies carried out in recent decades. Following these experimental studies, a typical hysteric curve showing pinching behavior of PCFT columns are derived. But up to the present, there is no accurate proposed FEM model that expresses the typical hysteretic behavior of PCFT columns. This is due to lack of accurate constitutive model of steel and concrete together with proper steel-concrete interaction model. Following these limitations, some scopes and goals are established for this research.

Chapter 2 (Theoretical background of material and interface models): Thin-walled tubular columns with in-filled concrete under cyclic loading exhibits complicated behavior accompanying local buckling and their hysteretic behaviors are strongly influenced by the behavior of the thin-walled hollow steel tube, confined in-filled concrete and steel-concrete interaction. The use of an accurate constitutive model to express the cyclic behavior of the material steel and concrete as well as proper interface modeling between tubular columns and in-filled concrete will be an only versatile method to compute the hysteretic behavior of PCFT columns. To express cyclic strain hardening, the modified 3-surface cyclic plasticity model is used herein as constitutive model for material steel, while concrete damaged plasticity model is used to simulate cyclic strain hardening, strain softening and brittle behavior of in-filled concrete. The inelastic behavior of concrete defined in this model is based on plasticity and damaged mechanics along with dilation characteristics of concrete material. The in-filled concrete imparts stiffness to the structure when steel-concrete interaction is possible. To express the contact with friction behavior along steel-concrete interface, an accurate modeling as well as approximate modeling is proposed. Hard contact and Coulomb friction model are considered as an accurate interface model, while bi-linear spring model for contact behavior and linear spring model for shearing behavior are referred

as approximate model for steel-concrete interaction. These two modeling are used to verify interface modeling effect on hysteretic behavior of PCFT columns.

Chapter 3 (Nonlinear FEM Analysis of CFT Columns): This chapter demonstrates details the 3-D FEM model to compute the hysteretic behavior of PCFT columns. The FEM model is determined based on the PCFT column specimens used in the unidirectional cyclic loading experiments carried out by the Public Work Research Institute, Japan. In this study, 4 types of FEM models are proposed for PCFT column specimens, based discrete crack location and type of interface modeling used for steel-concrete interaction as well as constitutive model used for in-filled concrete. To construct the FEM model, 4-node double curve general-purpose shell element with reduced integration (S4R) for steel tube and 8-node solid element with reduced integration (C3D8R) are used for concrete core. With considering geometric and material nonlinearity, the numerical analysis is carried out by using the general-purpose finite element package program ABAQUS. A comparison between the 4 types of FEM models is shown in order to investigate the hysteretic behavior of PCFT columns with considering interface modeling, discrete crack location and concrete constitutive model, and finally the most accurate and stable FEM model is proposed. The accuracy of the proposed FEM models is confirmed by comparing the computed results with the results of conventional cyclic loading experiments. Based on the proposed FEM model, the mechanical properties of PCFT column is investigated considering in-filled concrete restraining effect on tubular local buckling, strength, ductility and energy dissipation capacity of PCFT and corresponding hollow columns, confining pressure distribution on in-filled concrete and its effect on concrete strength as well as occurrence of metal fracture initiation in steel tube.

Chapter 4 (Summary): An accurate and numerically stable FEM model is proposed for PCFT columns in this study. The hysteretic behavior of PCFT columns obtained from proposed model shows pinching hysteretic loop characteristics that observed in the unidirectional cyclic loading experiments. The present analytical study is mainly concerned with the computation of hysteretic behavior of PCFT columns under cyclic unidirectional load. But, to ensure the safety of elevated highway bridges under earthquake waves, it is necessary to compute bi-directional hysteretic behavior of PCFT columns. In this respect, some scopes are recommendations are proposed for future research.

NOTATIONS

Roman Upper Case Letters

D	Diameter of the steel tube
E_c	Concrete Young's modulus
E_s	Steel Young's modulus
H_m^p	Plastic hardening modulus
H	Horizontal reaction force
H_0	Initial horizontal yield force
K_c	Yield surface roundness parameter
D_o^{el}	Initial elastic stiffness tensor
R_t	Radius to thickness ratio parameter
A_E	Plastic energy dissipation

Roman Lower Case Letters

p	Contact pressure
d_c	Compressive damage variable
d_t	Tensile damage variable
$f_c^{/}$	Uniaxial compressive strength of concrete
q	Mises equivalent stress
t	Thickness of the steel tube
h	Height of the column
h_c	Height of in-filled concrete
f_b	Minimum radius of contracted yield surface
$w_{c,t}$	Stiffness recovery factor
k_r, k_z, k_θ	Spring constant

Greek Letters

$\bar{\sigma}$	Effective stress tensor
σ_{b0}	Biaxial yield stress
σ_{t0}	Uniaxial tensile strength of concrete
$\hat{\bar{\sigma}}_{\max}$	Effective maximum principal stress
σ_y	Steel yield strength
σ_u	Tensile strength of steel

ν_c	Concrete Poisson's ratio
ν_s	Steel Poisson's ratio
e	Eccentricity of failure surface
ψ	Dilation angle
μ	Friction coefficient
$\varepsilon_{c,t}$	Total strain
$\tilde{\varepsilon}_c^{in}$	Inelastic strain
$\tilde{\varepsilon}_{c,t}^{pl}$	Equivalent plastic strain
α, β, γ	Yield coefficient
τ_{cr}	Critical shear stress
τ_Σ	Resultant shear stress
δ	Horizontal displacement
δ_0	Initial yield displacement
ε_{yp}	Original length of yield plateau
β	Elastic range reduction rate
ρ	Elastic range expansion coefficient
κ	Discontinuous coefficient
ξ	Curve-fitting parameter
$\bar{\lambda}$	Slenderness ration parameter

Abbreviations

c	Compression
t	Tension
FEM	Finite element method
CFT	Concrete filled steel tube
PCFT	Partially concrete filled steel tube

Chapter 1

Introduction

1.1 General

Partially concrete-filled thin-walled steel tubular columns referred hereinafter as PCFT columns are often preferred as elevated highway bridge piers (**Fig.1-1**) in urban areas, Japan. In 1995 Kobe earthquake, most of highway bridge piers are severely damaged due to local buckling of tubular columns (**Fig.1-2**). Considering the lessons learned from the Kobe earthquake, the Japanese seismic design code (Japan Road Association 2002) for highway bridges adopted a new design concept where the damage of the columns is controlled such that their residual deformation under the in-put earthquake waves becomes within an allowable value. However, the effects of local buckling on their strength and ductility must be carefully considered for the design of these piers. Therefore, it is important to predict accurately the ultimate behavior of PCFT columns during severe earthquakes.

The PCFT columns can be treated as an earthquake resistant structure, in which steel tube acts compositely with in-filled concrete such that the stiffness and load carrying capacity of the structure are significantly improved comparing with hollow columns. The concrete partially filled at lower part of hollow columns and confined by a diaphragm (**Fig.1-3**) is expected to improve the ductility & strength of hollow tubular columns without so much increasing the seismic inertia force. In PCFT columns, steel tube is expected to carry stresses primarily in the longitudinal direction caused by axial loading and moments, as well as in the transverse direction caused by shear and internal passive pressure due to concrete dilation. This can prevent the inward buckling of the steel tube and increase the stability of the structure. In addition, increasing the concrete strength due to confining pressure takes an important role to improve the performance of hollow columns. So, PCFT column offers very competitive solution comparing to the conventional RC column. This system is a completely new approach that is widely used in Japan, China and many other countries of the world. So, analysis and design of PCFT column is not only a special field of interest but also demandable from safety and economical points of view.

Fig.1-1 Elevated highway bridge pier used in the urban areas, Japan

(a)

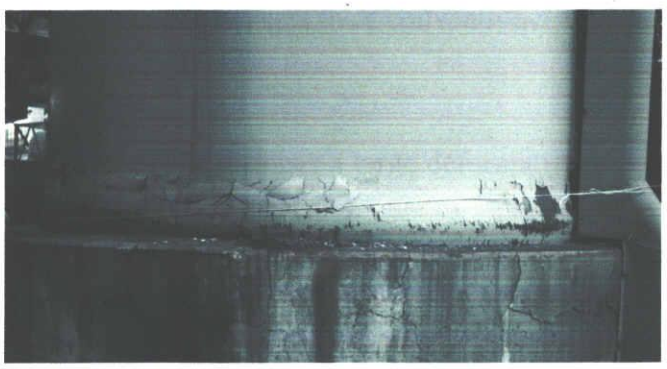

(b)

Fig.1-2 (a) Damage in highway bridge pier, (b) Damage occurred in a cylindrical pier due to 1995 Kobe Earthquake

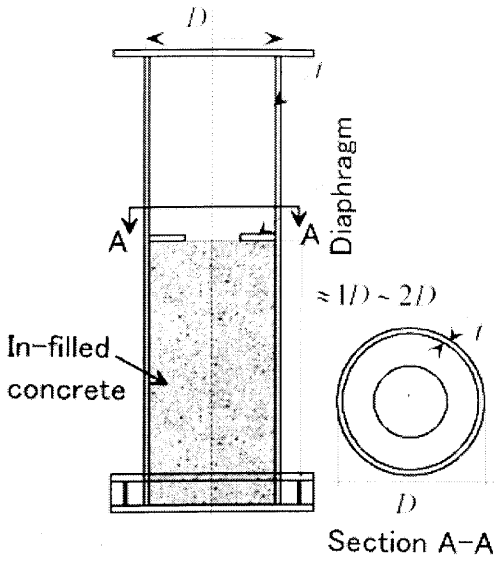

Fig.1-3 Definition of PCFT column model

1.2 Advantages of CFT columns

Japan is an earthquake-prone country where earthquake caused miserable disasters in different areas in recent years. It damaged an enormous number of railway constructions such as elevated RC and steel bridges. Thereafter, CFT column draws attention as a structural member of high resistibility to the earthquake. The composite action of CFT column gives relatively better advantages over conventional steel or reinforced concrete column. The advantages are enlisted below.

i) Concrete filled steel tubular column has a large deformation capacity combining steel and concrete rationally.
ii) It shows good performance on the durability compared with hollow tubular columns.
iii) It is becoming increasingly popular in structural applications around the world due to their excellent earthquake resistant properties such as small cross sectional area, high strength, high ductility, large energy absorption capacity.
iv) The composite column helps to control lateral drift and local buckling of steel tube is delayed due to steel-concrete surface interaction and dilation of in-filled concrete.
vi) Moreover, the steel tube encloses the concrete core and can be used as both longitudinal and lateral reinforcement as well as formwork during casting of concrete. This type of column can offer many other advantages, for instance the increased speed of construction, better safety and deducing construction expenses of public work

required for economic design.

1.3 Common difficulties to analyze the CFT columns

It is well recognized that the proper use of two or more material in structures generally leads to a more efficient and economical systems for resisting seismic load. In this regard, CFT is an innovative idea, which is finding increasing applications in design practice. In spite of excellent advantages, designers rarely utilize CFT system, since few practical nonlinear FEM models have been developed to simulate the important aspects of CFT column. In contrast, relatively few researchers have developed an efficient method to study the load-deformation behavior of CFT column subjected to cyclic loading. This is partly because severe discontinuity occurs to compute numerical analysis. This discontinuity arises from material nonlinearity and steel-concrete contact interface. The interface opening and closing through height of the column changes rapidly and causes severe contact problem for FEM analysis. To overcome this problem, it will be essential to model the interface action along with the local buckling of steel tube and nonlinear behavior of confined concrete accurately.

1.4 Typical hysteretic behavior of PCFT columns

According to the results of the unidirectional cyclic loading test (Public work research institute, 1997-2000, Iura et al. 2002), PCFT columns exhibit a characteristic pinching hysteresis loop shown in **Fig. 1-3**, expressed in terms of horizontal load-displacement relationship. The typical hysteretic behavior of PCFT columns has two distinct features. First, the hysteresis loop shows a recovery of stiffness in the loading process. This may be explained by the opening and subsequent closing behavior of concrete cracks transverse to the column axis. When the horizontal displacement approaches zero, the cracks that are closed in the compression side open due to the decrease of the compressive stress. This results in the stiffness degradation. However, when the horizontal displacement increases from zero in the opposite direction, the cracks again close on the compressive side and the column recover its stiffness. Second, being different from the RC columns, the energy dissipation capacity of the hysteresis loop is rather stable, regardless of the magnitude of the amplitude. This is because the local buckling of the steel tube is restrained by the confined concrete. There are several parameters of steel and concrete materials influencing to develop the pinching behavior of PCFT column, such as dilation of in-filled concrete, steel-concrete initial interface

clearance, confining pressure, biaxial stress ratio. The confining pressure induced from steel tube is directly related to concrete dilation as well as steel-concrete interface clearance and takes an important role in crack opening and subsequent crack closing of concrete. Regarding steel material parameters, initial length of yield plateau and radius of contracted yield surface takes important role in developing pinching hysteretic loop characteristics of PCFT columns. In this study, such kind of pinching behavior is examined by experimentally and a numerically stable FEM model is proposed to access hysteretic behavior of PCFT columns.

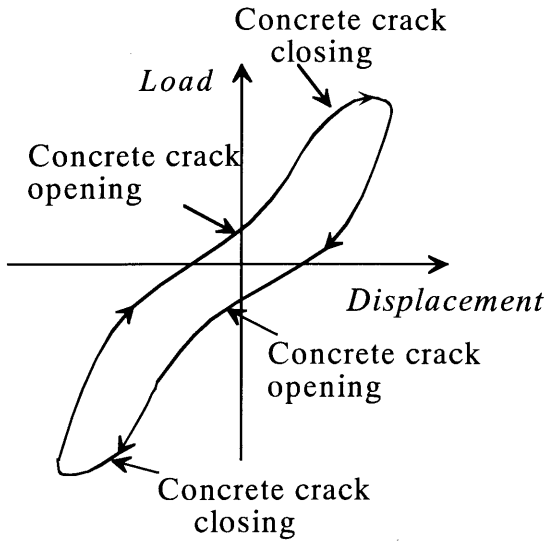

Fig. 1-4. Hysteretic curve showing pinching behavior of PCFT column.

1.5 Background of the present study on CFT columns

The PCFT columns under cyclic loading exhibit complicated behavior accompanying with local buckling of steel tube and concrete cracking. But up to now, extensively limited researches on PCFT columns are not capable to predict the ultimate seismic behavior accurately.

Experimental study

In recent decades, several experimental studies (Iura et al. 2002, Morishita et al. 2000, Hanbin Ge et al. 1996 and Public Work Research Institute, 1997-2000, among others) have been conducted to examine the hysteretic behavior of PCFT columns. Furthermore, these experimental studies are mainly focused on the behavior of PCFT column under cyclic unidirectional load. However, up to the present, there are no

experiments on PCFT columns to compute the hysteretic behavior under bidirectional cyclic loading. But the severest bidirectional cyclic loading has an unfavorable effect on strength and ductility of PCFT columns.

Analytical study

The geometrical and material nonlinear FEM analysis may be a versatile method in predicting the hysteretic behaviors of CFT bridge piers, which are mainly affected by cyclic plasticity of steel tube with local buckling, inelasticity of confined in-filled concrete and interaction between steel tube and in-filled concrete. Regarding the geometric and material nonlinear analysis, some analytical approaches have been proposed following the above mentioned cyclic unidirectional experimental studies. These analytical models have been proposed to predict the hysteretic behavior of PCFT columns in an indirect manner and are basically based on beam theory (Susantha et al. 2002, Varma et al. 2002). However, these models basically intended for practical design use are not capable of considering properly the local buckling of thin-walled steel tube along with the interaction between steel tube and in-filled concrete.

Matsumura et al. (2003) proposed a 3-D analytical model where the steel tube and in-filled concrete are represented by geometrically and materially nonlinear shell elements and solid elements, respectively. In their model, the contact behavior between steel tube and in-filled concrete is considered, although the interface friction in the tangential direction is ignored. The application of their model is limited only to the behavior under monotonic loading due to some numerical problems. The post-peak behavior of the CFT column predicted by the model differs significantly from the existing experimental results.

Fujii et al. (2003) used a FEM model similar to Matsumura, although the constitutive model for in-filled concrete and the modeling of the interface action is simplified. That is, an elastic-perfectly plastic model is used for the in-filled concrete and a contact elastic spring model is used for the interface. The contact spring elements are inserted at the initial state and their locations are assumed not to change during the subsequent loading. Probably because of these simplified models, the pinching hysteretic loop characteristics of the CFT columns are not obtained in their analysis.

Hsu et al. (2003) also presented a FEM model similar to Fujii et al. (2003). However, they disclose neither the constitutive models nor the interface model. The application of their model is limited only to the analysis of the local buckling pattern under monotonic loading.

The previous studies on CFT column are mainly focused on two important aspects: simple constitutive model for in-filled concrete and relatively approximate interface modeling. Therefore, accurate interface and material modeling will be a direct approach to compute the hysteretic behavior of PCFT columns.

1.6 Objective of this study

To get better understanding the mechanical behavior of concrete filled steel tubular columns, it is necessary to draw attention to behavior of steel tube with local buckling, inelastic behavior of in-filled concrete with confining effect and interaction between steel tube and in-filled concrete. In the previous analytical studies, most attention was given to the behavior of the steel, and the concrete was very often treated just as a way to strengthen and stabilize the steel member. But concrete shows complex inelastic behavior under confining pressure. Therefore, it is necessary to propose an accurate analytical approach to compute hysteretic behavior of PCFT columns with considering accurate concrete model as well as proper interaction model between steel tube and in-filled concrete. To achieve this goal, following scopes are taken into consideration for the present study.

First, the cyclic local buckling of thin-walled steel tube that usually governs their ultimate behavior is prevented by the internal passive pressure due to the dilation of in-filled concrete. On the other hand, this pressure that acts as confinement to the in-filled concrete also increases the strength of concrete. Therefore, accurate modeling of the interface action together with the behavior of confined concrete and thin-walled steel tube may be an only versatile method to predict the hysteretic behavior of PCFT columns in a direct manner. The objective of the present study is to propose a more accurate, yet numerically stable FEM model that considers geometric and material nonlinearity. The accuracy of the proposed model is to be verified by comparing the computed results with the results of cyclic loading experiments.

Second, the failure mechanism of PCFT columns comprises the occurrence of metal fracture in steel tube and confining pressure distribution on in-filled concrete. In PCFT columns, steel tube goes to large inelastic deformation under cyclic loading. However, the metal fracture is likely to form in steel tube where local buckling occurs. On the other hand, in-filled concrete suffers from complicated confining pressure distribution

that generated from outer steel tube. Therefore, second objective of this study is to investigate these mechanical properties of PCFT columns.

Third, inward local buckling of steel tube is restrained by dilation of in-filled concrete and steel-concrete interaction. In this study, it will be investigated how in-filled concrete restraining effect significantly improves the strength, ductility and energy dissipation capacity of PCFT columns, comparing with corresponding hollow columns.

Chapter 2

Theoretical background of material and interface models

2.1 General

Hysteretic behavior of PCFT columns is strongly influenced by the behavior of the thin-walled hollow steel tube, confined in-filled concrete and steel-concrete interaction. Therefore, it is necessary to use an accurate constitutive model to express the cyclic behavior of the material steel and concrete as well as appropriate interface modeling. Steel is assumed to be initially elastic with strain hardening capabilities after yielding. To express cyclic strain hardening, modified 3-surface cyclic plasticity model is used herein as constitutive model for material steel.

Under compression, the in-filled concrete behaves like a strain hardening material before crushing and strain softening material after crushing, and it shows brittle behavior under tension. To simulate this type of complex behavior, the damaged plasticity model based on plasticity with damage mechanics, is used as constitutive model for in-filled concrete. In this model, concrete hardening behavior is associated with both damage and plasticity, while softening behavior is controlled by damage mechanics only. However, this damage mechanics influences size of the yield surface as well as unloading process. The distinct feature of the model is the use of the inelastic surfaces that can be used to calculate plastic deformation. This constitutive model accounts essential properties of concrete material: strain hardening and strain softening behavior, dilation angle, shape of the yield surface, stiffness degradation and bi-axial stress ratio. The simultaneous use of plasticity and damage surface together with dilation characteristics of concrete material leads to be an accurate constitutive model for concrete material.

In PCFT columns, the in-filled concrete takes an important role in gaining strength when steel-concrete interaction is possible. The in-filled concrete imparts stiffness to the structure when they are in contact condition. This contact behavior is simulated by contact with friction model. The details of these two material constitutive models along with interface model are described in the following sections.

2.2 Modified 3-surface cyclic plasticity model for steel

Hysteretic behavior of PCFT columns is strongly influenced by the behavior of the thin-walled hollow steel tube. Therefore, it is necessary to use an accurate constitutive model to express the cyclic behavior of the material steel. Herein, the modified 3-surface cyclic plasticity model developed by Goto et al. (1998, 2006) is adopted as a constitutive model. This model can accurately analyze the hysteretic behavior of thin-walled steel columns under large equivalent plastic strain. There are three surfaces existing in the stress space: yield surface, discontinuous surface and bounding surface. The bounding surface is fixed in stress space and the radius of bounding surface is equal to ultimate tensile strength σ_u obtained from tensile coupon test. The discontinuous surface coincides with yield surface originally and expands isotropically at the initiation of strain hardening. This 3-surface cyclic plasticity model takes into account the important characteristics of cyclic steel plasticity with less parameters and internal variables such as the effects of yield plateau, contraction of elastic range and cyclic strain hardening. The modified 3-surface model is described details elsewhere by Goto et al. (1998, 2006) and shown schematically in **Fig.2-1**.

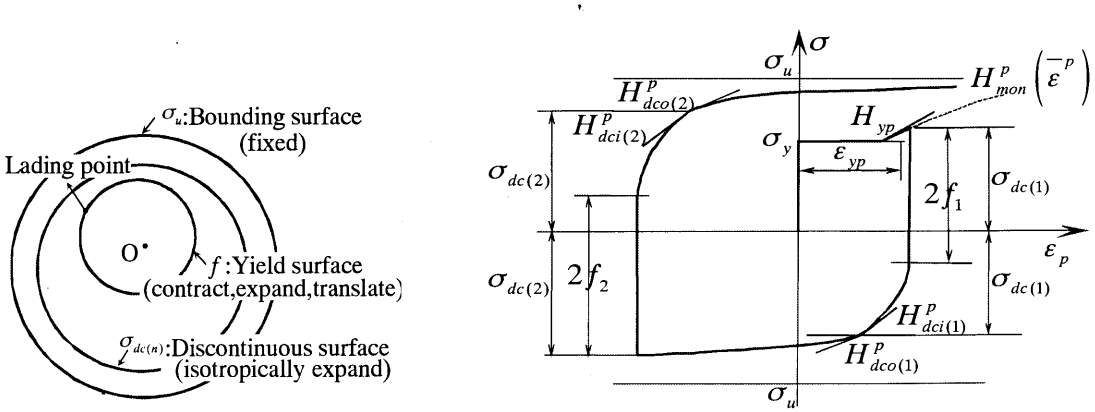

(a) Multiaxial stress space representation (b) Uniaxial stress-strain relation

Fig.2-1 Modified 3-surface model under cyclic load

The 3-surface cyclic plasticity model introduces ten material parameters for steel, such as Young's modulus E_s, Poisson's ratio υ_s, yield stress σ_y, ultimate tensile stress σ_u, original length of yield plateau ε_{yp}, plastic modulus H_m^p obtained by tensile coupon test, minimum radius of contracted yield surface f_b, elastic range reduction rate β, elastic range expansion coefficient ρ, discontinuous coefficient κ and curve-fitting parameter ξ for tensile coupon test. The parameters defined above are to be calibrated from tensile coupon test results along with the cyclic loading experiments on thin-walled hollow steel columns (Goto et al, 1998, 2006). The modified 3-surface model is implemented in the general purpose finite element package program ABAQUS ver.6.6 by USER SUBROUTINE feature. For a specified strain increment, USER SUBROUTINE is made such that stress increment is calculated by the modified 3-surface model.

2.3 Concrete material model

As is well known, the constitutive relation of in-filled concrete influences the stability of the numerical calculation. In recent years, Finite Element Method (FEM) has emerged as the most powerful general method of structural analysis and has provided engineers with a tool of very wide applicability. Indeed, FEM now offers a powerful and general analytical tool for reinforced concrete members and structures. Concrete cracking, tension stiffening, compressive hardening and softening, so called multiaxial nonlinear behavior can be modeled virtually by FEM analysis. The following sections represent different concrete material models with their advantages, drawbacks, and limitations in application.

2.3.1 Review of concrete material models

An isotropic hardening model proposed by Chen and Chen (1975a) applicable for triaxial state under simple loading condition. This model is based on associated flow rule and provides no idea about strain softening behavior of concrete. The crushing type failure occurs while stress state exceeds the ultimate strength value and concrete loses its strength completely. Although this model is applicable for triaxial case, but no consideration related to triaxial effect was taken into account in loading function. However, when concrete will be subjected to triaxial state and laterally confined, it will not be capable to control volume dilation. Therefore, concrete will behave in

discontinuous manner and numerical analysis will be unstable under complex loading.

Darwin and Pecknold (1977) proposed an orthotropic hypo-elastic model based on equivalent stress-strain concept and material parameters are obtained from equivalent uniaxial curve. Toader et al. 1997 modified the hypo-elastic model and applied in triaxial stress state under cyclic loading. The directions of orthotropy were assumed to coincide with current principal stress directions according to the rotating smeared-crack approach. This model considers nonlinear stress-strain behavior, tensile cracking, compression crushing and strain softening. The principal characteristic of these models is that inelasticity does not depend on flow rule. Toader also recommends that this model may encounter some numerical convergence problem in a particular case of non-proportional loading. Abdelhafid et al. 1997 further modified this model introducing a normalized scalar damage parameter applied in unloading process for non-proportional loading. As is well known computing confining pressure is a complex phenomenon especially for structures subjected to bending. This factor is not considered in this model. All these sensitive and critical problems can be overcome by the use of non-associated flow rule that is the choice of a plastic potential distinct from the yield function. In addition, effective stress area and stiffness recovery concept are used to define concrete damaged plasticity model, which indirectly improve the computational efficiency. So, this model will be a suitable example that can overcome all problems mentioned above.

2.3.2 Concrete damaged plasticity model

Concrete that exhibits brittle behavior for tensile and small compressive stresses becomes ductile in presence of high hydrostatic pressures. The brittle behavior of concrete disappears when the confining pressure is sufficiently high to prevent crack propagation. Under these circumstances, a failure driven by the collapse of concrete microporous structures exhibits a macroscopic response that resembles the behavior of a ductile material. Therefore, in the conventional triaxial concrete models, the behavior under compressive stresses is represented by plasticity model, while the behavior under tensile and small compressive stresses is expressed by smeared cracking model. This model, however, often encounters numerical difficulty under cyclic load, when applied to FEM. To circumvent this situation, the concrete damaged plasticity model (Lee et al. 1998) implemented in ABAQUS is used herein. Although this is a thoroughly plastic model more approximate than the above-mentioned conventional model, better numerical stability is ensured. To simulate this complex behavior, a proper and

appropriate yield criterion is essential. Brittle and ductile models can be combined to provide a proper description of the post failure behavior of concrete in the ductile-brittle state. The main advantage of this model is that it can easily solve the nonlinear problem arising from conventional concrete models. This model is suitable for the analysis of concrete structures under monotonic /cyclic / dynamic loading. And unloading is possible to take place in a direction parallel to the initial stiffness or in any desired direction. The key point different yield strengths in tension and compression with significant amount of initial yield stress are considered in this model.

The constitutive relation is based on theory of plasticity and continuum damage mechanics. A simple scalar damage variable used in this model degrades the elastic stiffness due to crack opening, and recovers the stiffness after cracks closing. The use of multiple hardening variables used to define yield surface of concrete represents tensile and compressive damage independently. This constitutive model is based on damaged plasticity of concrete, which can lead to a decoupled algorithm for the effective stress computation and stiffness degradation evaluation. This model can effectively evaluate the irreversible damage of concrete under fairly low confining pressure (less than four or five times uniaxial compressive strength of concrete).

Concrete damaged plasticity model is an isotropic model and resembles with Drucker-Prager type model in the context of compressive behavior of concrete. This model is implemented to FEM by using 8- node solid element with reduced integration (C3D8R). It considers stiffness degradation and stiffness recovery due to the crack opening and crack closing of concrete, respectively. Damage associated with the failure mechanisms of the concrete results in a reduction in the elastic stiffness. The constitutive relation used in this model is expressed in Eq. (2-1).

$$\sigma = (1-d)D_0^{el} : (\varepsilon - \varepsilon^{pl}) \tag{2-1}$$

Where, σ = Cauchy stress tensor, ε = total strain tensor, ε^{pl} = plastic strain tensor (damaged plastic strain), D_0^{el} = initial elastic stiffness tensor. The stiffness degradation is isotropic and characterized by a single damage variable, d. The damage variable can take values from zero representing the undamaged material, to one representing total loss of strength. This damage variable can be defined in Eq. (2.2) in terms of both tensile and compressive damage variables.

$$1-d = \{1-(1-w_t)d_c\}\{1-(1-w_c)d_t\} \tag{2-2}$$

Here, d_c = compressive damage variables, d_t = tensile damage variables. Both variables take values from 0 to 1. However, two variables $\tilde{\varepsilon}_c^{pl}$ and $\tilde{\varepsilon}_t^{pl}$ used to define hardening behavior of concrete are assumed to be functions of these two damage parameters. Furthermore, Another two stiffness recovery factor is considered in this model, such as tension stiffness recovery factor w_t and compression stiffness recovery factor w_c. In general, the compressive stiffness of concrete is fully recovered as loading changes from tension to compression, i.e., $w_c = 1.0$. On the other hand, the stiffness is not recovered as loading changes from compression to tension, which corresponds to $w_t = 0.0$.

In damaged plasticity model, effective stress tensor $\bar{\boldsymbol{\sigma}}$ is expressed in terms of undamaged elastic stiffness tensor and scalar damage variable d, which is illustrated in Eq.(2-3).

$$\bar{\sigma} = (1-d)D_0^{el} : (\varepsilon - \varepsilon^{pl}) \tag{2-3}$$

From the above two equations Eq(2-2) and (2-3), the relation between effective stress tensor and Cauchy stress tensor can be expressed as $\sigma = (1-d)\bar{\sigma}$.

2.3.2.1 Yield function

The damaged plasticity model uses a yield function to account for different evolution of strength under tension and compression. In terms of effective stresses, the yield function F is expressed by using two hardening variables, $\tilde{\varepsilon}_t^{pl}$ and $\tilde{\varepsilon}_c^{pl}$ in Eq. (2-4).

$$F(\bar{\sigma}_i^{(n+1)}, \tilde{\varepsilon}_j^{pl(n+1)}) = \frac{1}{1-\alpha}\left(\bar{q} - 3\alpha\bar{p} + \beta(\tilde{\varepsilon}^{pl})\left\langle\hat{\bar{\sigma}}_{\max}\right\rangle - \gamma\left\langle-\hat{\bar{\sigma}}_{\max}\right\rangle\right) - \bar{\sigma}(\tilde{\varepsilon}_c^{pl}) = 0 \tag{2-4}$$

Here, $\langle.\rangle$ is the Macauley bracket defined by $\langle x\rangle = (|x| + x)/2$ and the coefficients of yield function are given by

$$\begin{aligned} &\alpha = \frac{(\sigma_{b0}/\sigma_{c0}) - 1}{2(\sigma_{b0}/\sigma_{c0}) - 1}; \quad 0 \le \alpha \le 0.5 \\ &\beta(\tilde{\varepsilon}^{pl}) = \frac{\bar{\sigma}_c(\tilde{\varepsilon}_c^{pl})}{\bar{\sigma}_t(\tilde{\varepsilon}_t^{pl})}(1-\alpha) - (1+\alpha); \quad \gamma = \frac{3(1-K_c)}{2K_c - 1} \end{aligned} \tag{2-5}$$

Where, $\bar{\sigma}_c(\tilde{\varepsilon}_c^{pl})$ and $\bar{\sigma}_t(\tilde{\varepsilon}_t^{pl})$ are effective compressive and tensile stress, respectively.

$\hat{\bar{\sigma}}_{max}$ is the maximum principal effective stress that defines the tensile and compressive criteria and and σ_{b0}/σ_{c0} is the biaxial stress ratio. A plane stress cross section of the yield surface in the principal stress space in shown in **Fig.2-2.**

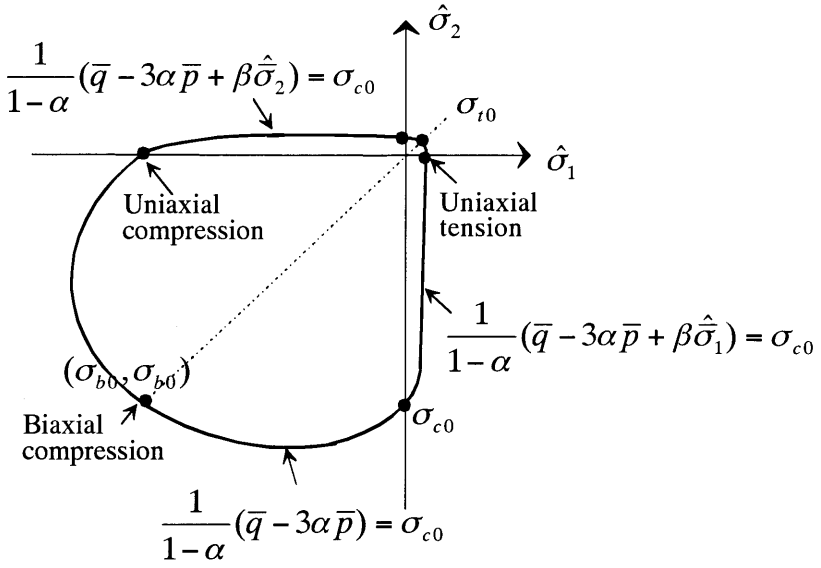

Fig. 2-2 Yield surface in plane stress space

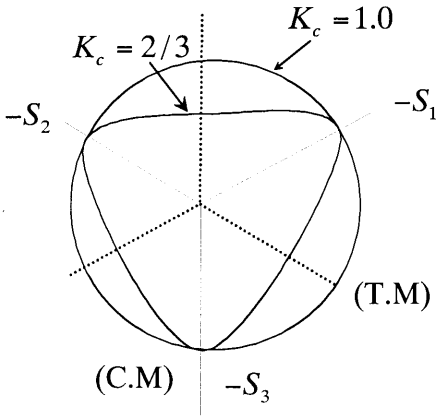

Fig. 2-3 Yield surfaces in the deviatoric plane, corresponding to different values of K_c

In Eq.(2-4), $\bar{q}_t$ and $\bar{q}_c$ expresse Mises equivalent effective stress for tensile and compressive meridian, respectively. The shape factor of yield surface is defined as $K_c = \bar{q}_t / \bar{q}_c$. The value of K_c ranges between 0 to 1. K_c = 1.0 implies that the yield surface is the Von Mises circle in the deviatoric principal stress plane in which yield stresses in triaxial tension and compression are the same. K_c = 0.5 implies that the yield surface is the Rankin's triangle in the deviatoric principal stress plane. When the value K_c increases, it expands the yield surface in deviation plane surface and forms to circle. While the value of K_c decreases, the size of the yield surface contracts and forms to regular triangular shape. A typical shape of yield surface is schematically shown in **Fig. 2-3** with different values of K_c.

2.3.2.2 Flow potential

The concrete damaged plasticity model is based on the non-associated flow rule, where the Drucker-Prager hyperbolic flow potential G is used to calculate plastic strain increment $d\varepsilon_j^{pl}$ as shown below.

$$d\varepsilon_j^{pl} = d\lambda \frac{\partial G}{\partial \bar{\sigma}_i}\Big|_{(n+1)} \tag{2-6}$$

$$G = \sqrt{(e\sigma_{t0}\tan\psi)^2 + \bar{q}^2} - \bar{p}\tan\psi \tag{2-7}$$

Where, ψ = dilation angle, σ_{t0} = tensile strength, $\bar{p} = -(1/3)trace(\bar{\sigma})$ = effective hydrostatic pressure. The function asymptotically approaches a linear flow potential **(Fig. 2-4)** at high confining pressure and intersects the hydrostatic pressure axis at 90^0. e is a parameter, referred to as eccentricity that defines the rate at which the function approaches the asymptote. The flow potential tends to be a straight line, as the eccentricity tends to zero. This flow potential is continuous and smooth, and ensures that flow direction is always uniquely defined. However, concrete damaged plasticity model uses different yield and potential function described above to define constitutive relation of concrete. The concrete model is integrated by using backward Euler method generally used for conventional plasticity model.

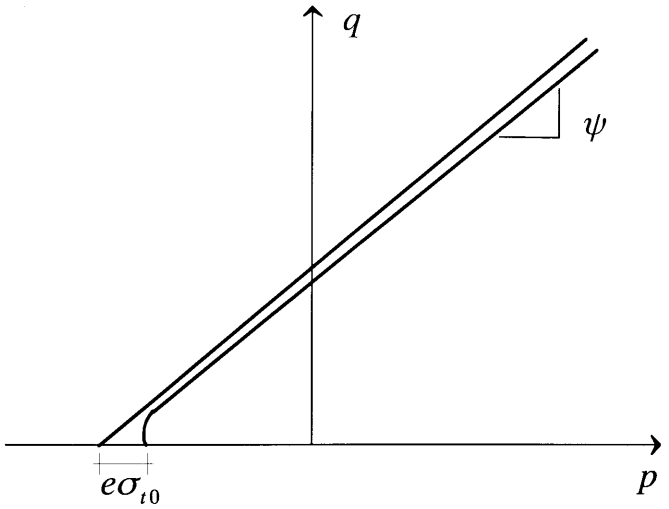

Fig. 2-4 Hyperbolic flow potential in p-q meridian plane.

In damaged plasticity model, the effective stress concept is used and defined as a function of equivalent plastic strain. Damaged states in tension and compression are characterized independently by two hardening variables, $\tilde{\varepsilon}_c^{pl}$ and $\tilde{\varepsilon}_t^{pl}$, which are referred to as equivalent plastic strain in compression and tension, respectively. From Eq. (2-6), eigen values of the plastic strain rate tensor $d\hat{\varepsilon}_i^{pl}(i=1,2,3)$ are determined. The principal incremental plastic strains components are ordered such that $d\hat{\varepsilon}_1^{pl} = d\hat{\varepsilon}_{\max}^{pl}$, $d\hat{\varepsilon}_2^{pl} = d\hat{\varepsilon}_{\text{mid}}^{pl}$ and $d\hat{\varepsilon}_3^{pl} = d\hat{\varepsilon}_{\min}^{pl}$. However, increment of two hardening variables $d\tilde{\varepsilon}_c^{pl}$ and $d\tilde{\varepsilon}_t^{pl}$ can be calculated from Eq.(2-8).

$$\begin{pmatrix} d\tilde{\varepsilon}_t^{pl} \\ d\tilde{\varepsilon}_c^{pl} \end{pmatrix} = \begin{bmatrix} r & 0 & 0 \\ 0 & 0 & -(1-r) \end{bmatrix} \begin{pmatrix} d\hat{\varepsilon}_1 \\ d\hat{\varepsilon}_2 \\ d\hat{\varepsilon}_3 \end{pmatrix} \tag{2-8}$$

where, $r(\hat{\bar{\sigma}})$ is stress weight factor defined in Eq. (2-9) and it becomes one if all principal stresses $\hat{\bar{\sigma}}_i(i=1,2,3)$, are positive and equal to zero if they are negative.

$$r = r(\hat{\bar{\sigma}}_i) = \frac{1}{2}\frac{\left|\hat{\bar{\sigma}}_1\right| + \left|\hat{\bar{\sigma}}_2\right| + \left|\hat{\bar{\sigma}}_3\right| + \hat{\bar{\sigma}}_1 + \hat{\bar{\sigma}}_2 + \hat{\bar{\sigma}}_3}{\left|\hat{\bar{\sigma}}_1\right| + \left|\hat{\bar{\sigma}}_2\right| + \left|\hat{\bar{\sigma}}_3\right|} \tag{2-9}$$

2.3.2.3 Concrete behavior under uniaxial compressive loading

The application of the concrete damaged plasticity model under uniaxial compressive load is expressed in **Fig. 2-5** in terms of stress-strain relation of plain concrete, which represents that concrete shows hardening behavior after initiation of yield stress and attains compressive strength $f_c^{/}$ at ultimate stage. Beyond this point, it goes to softening and fully crushes while stress becomes zero. To apply this model under uniaxial compressive load, it is necessary to compute hardening modulus from effective compressive stress $\bar{\sigma}_c$ and equivalent plastic strain $\tilde{\varepsilon}_c^{pl}$ relation obtained from uniaxial compression test on concrete cylinder specimen. The equivalent plastic strain is defined in Eq. (2-10).

$$\tilde{\varepsilon}_c^{pl} = \tilde{\varepsilon}_c^{in} - \frac{d_c}{(1-d_c)}\frac{\sigma_c}{E_c}; \qquad \text{where, } \tilde{\varepsilon}_c^{in} = \varepsilon_c - \sigma_c / E_c \tag{2-10}$$

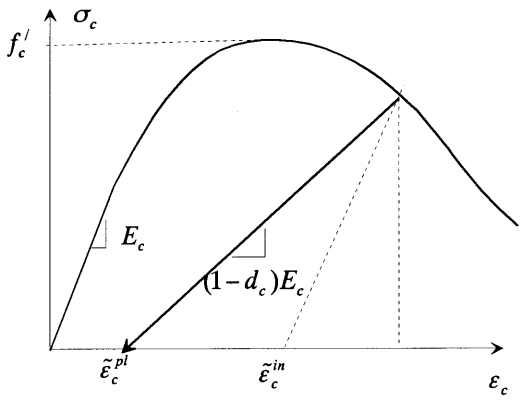

Fig. 2.5 Behavior of concrete under compression

2.3.2.4 Concrete behavior under uniaxial tensile loading

Generally, the behavior of concrete under tensile loading shows elastic stiffness up to maximum point and beyond the elastic limit, it goes into softening range. It is a usual assumption that forming cracks is a brittle process and the strength in the tensile loading direction gradually goes to zero after such cracks have formed. This tension softening behavior can be obtained from direct tensile test on concrete cylinder specimen. In damaged plasticity model, tensile behavior of concrete can be expressed by the tensile stress-strain relation, which is schematically shown in **Fig. 2.6**. In this model, the

inelastic cracking strain $\tilde{\varepsilon}_t^{in}$ is defined as the total strain minus the elastic strain corresponding to the undamaged material; that is, $\tilde{\varepsilon}_t^{in} = \varepsilon_t - \sigma_t / E_c$, and equivalent plastic strain for tensile case is calculated by using Eq. (2-11).

$$\tilde{\varepsilon}_t^{pl} = \tilde{\varepsilon}_t^{in} - \frac{d_t}{(1-d_t)} \frac{\sigma_t}{E_c} \tag{2-11}$$

Where, d_t is the tensile damage parameter. This tensile equivalent plastic strain $\tilde{\varepsilon}_t^{pl}$ is an important parameter to define the crack initiation and hardening variables. The tensile crack in concrete initiates when tensile equivalent plastic strain is greater than zero, $\tilde{\varepsilon}_t^{pl} > 0$.

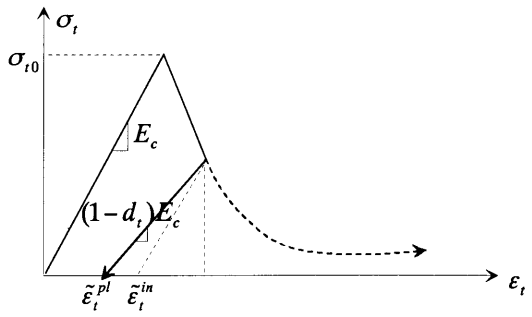

Fig. 2.6 Behavior of concrete under tension

The tension softening behavior of concrete is strongly influenced by the element size and cracking criteria will be different for elements with different sizes. However, it can be easily said that cracking criteria is associated with characteristics length L of element, which can be computed from cubic root of element volume. Therefore, with considering the element size effect on tensile softening behavior, tensile equivalent plastic strain can be calculated as $\tilde{\varepsilon}_t^{pl} = u^{cr} / L$, where u^{cr} is width of the concrete crack opening.

2.3.2.5 Concrete behavior under uniaxial cyclic loading

Under uniaxial cyclic loading, the behavior of concrete is strongly influenced by the opening and closing of previously formed micro-cracks. In damaged plasticity model, the microcrack opening and closing are simulated by degradation function, which is a

limitation of this model to express such discrete phenomenon. Moreover, there is some recovery of elastic stiffness when loading changes from tension to compression. This stiffness recovery concept is an important aspect under cyclic loading. The uniaxial stress-strain relation used in concrete damaged plasticity model under tension-compression-tension loading cycle is schematically shown by solid line in **Fig.2-7**. For comparison, the stress-strain relations under monotonic loading are illustrated by broken lines.

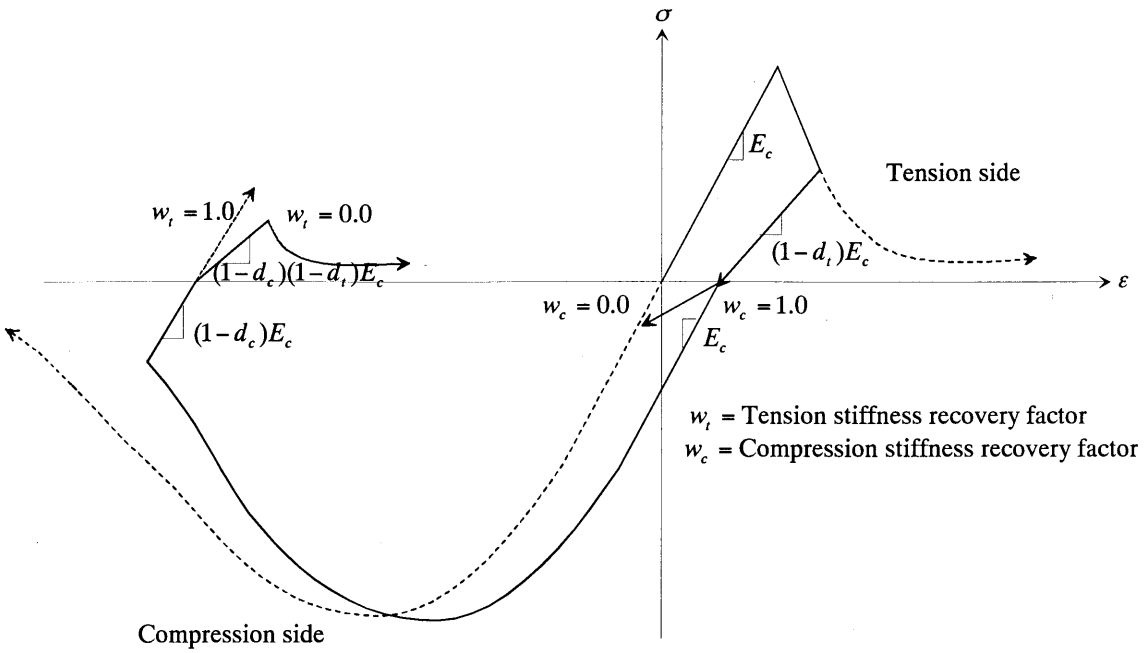

Fig. 2-7 Concrete model under cyclic loading

In damaged plasticity model, plasticity is calculated based on flow rule and only one yield function is used for both compressive and tensile case. That's why it ensures better numerical stability when applied to FEM, in comparison with smeared cracking model. But when concrete is subjected to cyclic loading, tension softening behavior defined in both two models does not exhibit the accurate crack opening and crack closing phenomenon occurred cyclically, which results in less accuracy of the numerical results. In this study, tensile behavior of concrete is replaced by discrete crack model, which is introduced in in-filled concrete as a discrete crack surface perpendicular to column axis and located at a place where relatively larger local deformation occurs in steel tube. Herein, the behavior of discrete crack in concrete is simulated with contact pair model. Therefore, discrete cracking model for tensile case along with damaged plasticity model for compressive case are used together to express the accurate constitutive relation of concrete.

2.4 Interface model

It is of great interest to know how the interaction between steel tube and in-filled concrete influences the structural behavior of CFT column. Herein, several distinct features are explained schematically in order to understand the interface behavior between tubular column and in-filled concrete.

2.4.1 Spring model

To simulate interaction between tubular column and in-filled concrete, spring element can be used as an interface element, although this is thoroughly an approximate model. The contact behavior between steel tube and in-filled concrete can be modeled with contact spring. When the interface element experiences tension, gap arises between tubular column and concrete, that is, no contact between them. On the other hand, when the clearance between two faces reduces to zero, contact forces acts at a point in normal direction. Fujii et al. 2003 expressed this contact behavior between steel tube and in-filled concrete by bi-linear contact spring model, which is schematically shown in **Fig.2-8**. In this model, the spring stiffness k_r for compression side is assumed to be relatively higher stiffness, while k_r for tension side is considered to be zero. In addition, when concrete surface comes into contact with steel surface and tends to slip with each other, shear force acts on their interfaces both in vertical and horizontal directions (k_z, k_θ), which results in resultant shear stress τ_Σ. In this study, this shearing behavior between tubular columns and in-filled concrete is simulated by linear shear spring model.

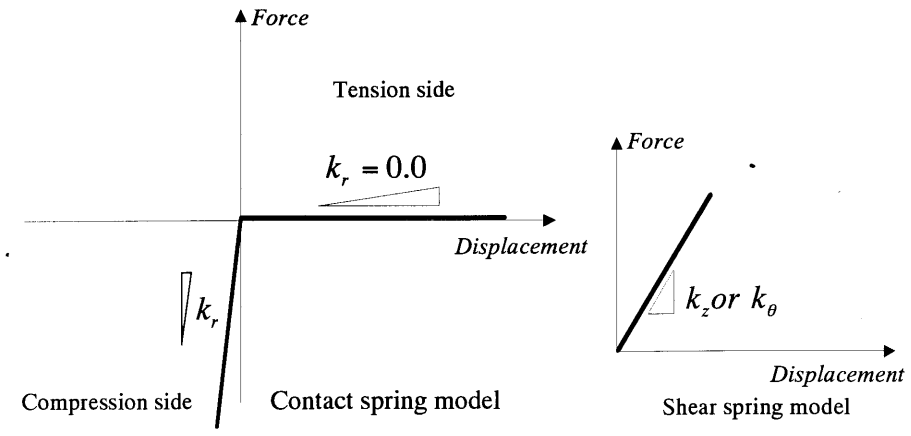

Fig.2-8 Spring model

In the above spring model, spring elements are inserted between steel-concrete interface and these are not allowed to change their original positions. But when large deformation occurs in tubular columns due to local buckling in steel tube, the spring

orientation will be changed and interface behavior completely differs from real case. If the resultant shear stress τ_{Σ} exceeds the limiting value of shear stress, concrete node slips along the surface of steel tube, and thereby, the shearing stiffness becomes zero. Such kind of phenomenon was ignored in the spring model proposed by Fujii. Due to this limitation in spring model, the post-peak behavior becomes larger comparing with the experimental results (Fujii et al. 2003).

2.4.2 Contact pair model

To overcome the limitation in spring model, another alternative approach is to use surface based interaction model, where special kind of algorithm is considered to simulate steel-concrete interface behavior and referred herein as an accurate interface model. Although sometimes it causes severe discontinuity between two contact bodies when contact node penetrates, which indirectly results in convergence problem for numerical analysis. The separated surfaces come into contact when clearance between them reduces to zero and contact pressure acts on the respective surfaces. The surfaces separate, if the contact pressure becomes zero. This contact behavior is simulated with 'hard contact' model implemented in ABAQUS. In this model, master and slave surfaces are referred to as contact pair (**Fig.2-9**). Generally, the master and slave surfaces should be chosen as the surface of the stiffer body and softening body, respectively. The surfaces are able to separate in a more realistic way and slide relatively to each other. Not only is that it possible to investigate the local buckling in steel section, separated from concrete core by surface based interaction.

Contact condition

i) Each potential contact condition is defined in terms of a slave node and a master surface.

ii) The contact direction is always normal to the master surface.

iii) In principle, the slave nodes are constrained not to penetrate into the master surface.

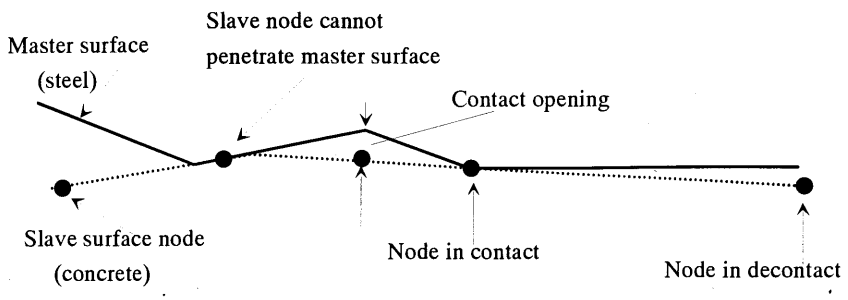

Fig.2-9 Contact pair

Coulomb friction model

When the slave node comes into contact with master surface, the contact pressure p occurs in the direction normal to the surface. At the same time, friction force occurs in the tangential direction. This friction behavior is simulated by 'Coulomb friction model' shown in **Fig.2-10**, where the resultant shear stress $\tau_{\Sigma} = \sqrt{(\tau_1^2 + \tau_2^2)}$ is computed from two orthogonal components of shear stresses τ_1 and τ_2, acting on the interface between two contact bodies. The friction model assumes that two contact surfaces can carry the resultant shear stress up to a certain magnitude at their interface before they start to slip. Thus, magnitude of the resultant shear stress is defined as critical shear stress τ_{cr}, which is proportional to contact pressure p and expressed in Eq. (2-12). The slip will occur along the interface when the shear stress reaches the critical stress ($\tau_{\Sigma} = \tau_{cr}$). In this case, constant shear stress ($\tau_{\Sigma} = \tau_{cr}$) acts at the interface during the slip. If $\tau_{\Sigma} < \tau_{cr}$, no relative motion occurs.

$$\tau_{cr} = \mu p \tag{2-12}$$

Where μ = friction coefficient between interface of the adjacent surfaces.

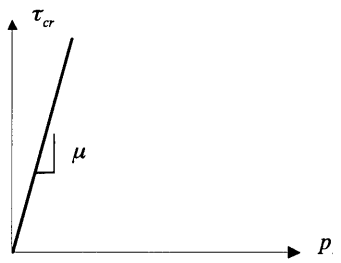

Fig.2-10 Coulomb friction model

Chapter 3

Nonlinear FEM Analysis of CFT Columns

3.1 General

In order to ensure the safety of CFT bridge piers during great earthquakes, it is necessary to examine their inelastic behavior under cyclic loading accurately (Japan Society of Civil Engineers (1996), Japan Road Association (1995)). The CFT bridge pier is composed of tubular columns and in-filled concrete. The ultimate seismic behavior of CFT bridge piers is strongly influenced by the material cyclic plastic behavior as well as the cyclic interaction between steel tube and behavior of in-filled concrete. In past, there are several cyclic unidirectional experimentas (Iura et al. 2002, Morishita et al. 2000, Hanbin Ge et al. 1996, Public work research institute, 1997-2000 and among others) carried out to examine the hysteretic behavior of CFT columns. These experimental investigations on ultimate behavior of CFT columns are undoubtedly a great help in clarifying their hysteretic behavior. Following these experimental studies, some analytical models based on beam theory have been proposed to predict the hysteretic behavior of CFT columns. But these models are not capable to analyse the post buckling behavior of CFT columns along with the interaction between steel tube and in-filled concrete. However, up to the present, no researches have been conducted to compute the hysteretic behavior of PCFT columns in a direct manner. This due to lack of accurate modeling of the behavior of in-filled concrete with confining effect as well as proper interaction model. Therefore, accurate modeling of the interface action together with the behavior of confined concrete and thin-walled steel tube may be an only versatile method to predict the hysteretic behavior of CFT columns in a direct manner. In this analysis, steel tube and concrete are represented by nonlinear shell and solid elements, repectively. To express the material behavior, the 3-surface cyclic plasticity model is used for steel tube, while the concrete damaged plasticity model is used for in-filled concrete. Contact and friction behaviors are considered for interface modeling. The accuracy of the proposed FEM model is herein examined by comparing the computed results with the results of conventional cyclic loading experiments.

3.2 Summary of the test specimens

A PCFT column model for the present analysis is illustrated in **Fig.3-1**. This model is determined based on the PCFT column specimens used in the unidirectional cyclic loading experiments conducted by the Public Work Research Institute. The PCFT column specimens are so-called a cantilever type with fixed base. The cyclic loading pattern used for specimens are explained in **Fig.3-2**. At the top of the specimen, alternating horizontal load under displacement control is applied with keeping the vertical load P constant.

The model specimens are made of carbon steel pipe (SS400) with 900 mm in diameter and 9 mm in thickness, and three diaphragms with 6 mm in thickness are welded to the inside of the pipe at an interval of 900 mm. The geometric and material parameters for the specimens are summarized in **Table 3-1**. Among these parameters, the radius-to-thickness ratio parameter R_t has a great influence on the local buckling behavior of PCFT columns. Herein, the model specimens (No.16, No.30 & No.29) have the same radius-to-thickness ratio parameter of $R_t = 0.123$. No.16 and No.30 are PCFT columns with different axial force ratio ($P/\sigma_y A$). No.29 has a hollow section without in-filled concrete.

Table 3-1 Geometric and material properties of the specimens

Specimen	No.16 (PCFT)	No.30 (PCFT)	No.29 (Hollow)
Material	SS400	SS400	SS400
Height,h (m)	3.423	3.423	3.423
hc (m)	2.303	2.303	-
t (mm)	9	9	9
Diameter,D (mm)	900	900	900
$\bar{\lambda}$	0.268	0.268	0.268
R_t	0.123	0.123	0.123
H_0(KN)	443.94	400.82	400.82
δ_0(mm)	11.53	10.5	10.5
$P/\sigma_y A$	0.114	0.199	0.199
f_c'(MPa)	27.93	21.46	-

Note: $\bar{\lambda} = \frac{2h}{\pi\sqrt{I/A}}\sqrt{\frac{\sigma_y}{E_s}}$ (slenderness ratio parameter),

$R_t = \frac{R}{t}\frac{\sigma_y}{E_s}\sqrt{3(1-\nu_s^2)}$ (radius-to-thickness ratio parameter),

$H_0 = (\sigma_y - P/A)Z/h$ (initial yield force),

$\delta_0 = H_0 h^3 / 3EI$ (initial yield displacement).

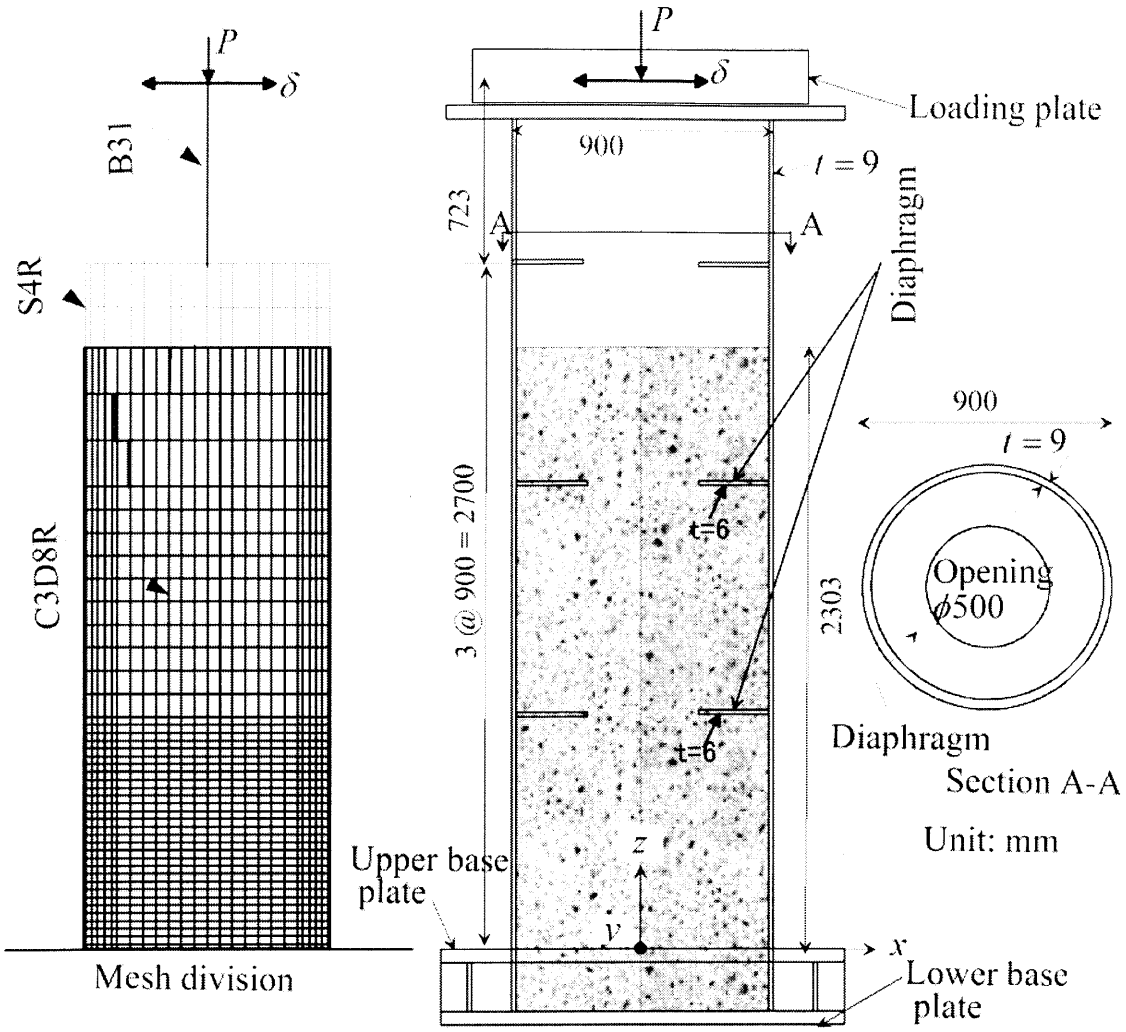

Fig. 3-1 Specimen and FEM model

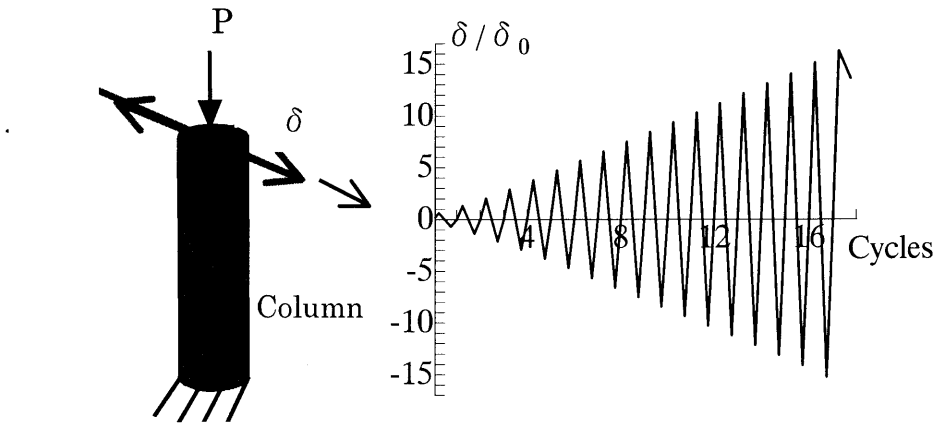

Fig. 3-2 Cyclic loading program

3.3 FEM modeling and material constants determination

In the FEM model, only half of the model is discretized by virtue of symmetry of the structure. Steel tube with diaphragms is modeled with the 4-node double curve general-purpose shell element with reduced integration (S4R). The lower part of column is discretized from fine mesh to relatively coarse mesh; while the upper part is modeled with elastic beam element with pipe section (B31).The concrete core is represented by the 8-node solid element with reduced integration (C3D8R). The numerical analysis considering the geometrical and material nonlinearity is carried out by using the general-purpose finite element package program ABAQUS ver. 6.6. Furthermore, the in-filled concrete is hardened before testing the PCFT column specimen and an initial gap between steel-concrete interfaces is generated due to dry shrinkage of concrete. Considering this point, an initial gap of 0.5 mm between tubular column and in-filled concrete is considered for numerical analysis. In this model, the applied axial load is distributed on in-filled concrete through two intermediate diaphragms.

3.3.1 Categories of analytical modeling

In this study, different four types of analytical modeling are used to determine the hysteretic behavior of thin-walled steel tubular columns filled with concrete. Analytical modeling categories are determined based on type of modeling used for interface between in-filled concrete and steel tube as well as diaphragm, and constitutive model for in-filled concrete. The analytical models are summarized in **Table 3-2**.

The 「Proposed model」 is a unique characteristic model and recommended to determine hysteretic behavior of PCFT columns when occurrence of concrete crack surface near the upper base plate dominates the pinching characteristics.

The 「Accurate model」 can be defined as a realistic model, where concrete crack surface generates at a possible location. However, this model is accompanied with occurrence of concrete crack surface near local buckling of tubular columns, where large inelastic deformation occurs.

The 「Boundary spring model」 is very close to 「Proposed model」 in context of discrete crack location and differs in the sense that the interface between in-filled concrete and steel tube is modeled by spring element. Rather, this modeling can easily overcome the interface contact problem and ensure better stability for FEM analysis. In this model, contact behavior is expressed by bi-linear contact spring, while interface shearing action is represented by linear shear spring.

Table 3-2 Concrete filled steel tubular column models

Model name	In-filled concrete		Boundary between steel tube and in-filled concrete	Steel tube
	Constitutive model	Location of discrete crack surface		
Proposed model	Damaged plasticity model	Above the upper base plate	Contact pair Coulomb's friction	3-surface model with shell element
Accurate model	Damaged plasticity model	At local buckling of steel tube	Contact pair Coulomb's friction	
Boundary spring model	Damaged plasticity model	Above the upper base plate	Contact spring Shear spring	
Elastic in-filled concrete model	Linear elastic model	Above the upper base plate	Contact pair Coulomb's friction	

The 「Elastic in-filled concrete model」 also introduces the discrete crack surface near upper base plate and inelasticity of in-filled concrete is ignored. The basis of this assumption is that the concrete partially filled at lower part of hollow columns is confined by a diaphragm and expected not to be severely damaged during earthquake. In this model, the in-filled concrete behaves like a linear elastic material and concrete damage is ignored.

In this study, computed hysteretic behaviors of PCFT columns considering with different FEM models and different interface modeling are to be compared. Therefore, parameters for 3-surface cyclic plasticity model and concrete damage plasticity model are to be determined with checking the minimum error. For this purpose, the experimental results of PCFT column No.30 and corresponding hollow column No.29 are used to calibrate the material parameters. Hence, the results of No.29 are used as a reference column to identify the steel material parameters for modified 3-Surface model, while the results of No.30 are used herein to calibrate in-filled concrete material parameters for damaged plasticity model. Lastly, determined and calibrated parameters for concrete and steel materials are confirmed by verifying the numerical results of the PCFT specimen No.16 with the results of the experiments.

3.3.2 3-surface model parameters calibration

There are a total of 10 parameters required to uniquely define the 3-surface model, that is: Young's modulus E_s, Poisson's ratio ν_s, yield stress σ_y, ultimate tensile stress σ_u, length of the original yield plateau ε_{yp}, plastic modulus in the hardening range under monotonic loading H_m^p, convergent elastic range f_b, elastic range reduction rate β, elastic range expansion coefficient ρ and discontinuous coefficient κ. The above material parameters except for f_b, β, ρ, and κ are determined from the conventional monotonic tensile coupon test results. Generally steel material shows hardening behavior beyond the yielding point and fracture occurs when strain at localized area exceeds the ultimate tensile strain. To express this inelastic behavior of steel material, JSCE Committee on Steel Structure (1996) has proposed an empirical formula, which is formulated in Eq.(3-1) in terms of nominal stress σ^{nom} and engineering strain ε^{nom} relation.

$$\sigma^{nom} = \frac{1}{\xi^*}\varepsilon_y^{nom} E_{yp}\left\{1-\exp(-\xi^*(\varepsilon^{nom}-\varepsilon_{yp}^{nom})/\varepsilon_y^{nom})\right\}+\sigma_y^{nom} \tag{3-1}$$

Where, curve shape factor ξ^* is calculated from Eq.(3-2)

$$\sigma_u^{nom} = \frac{1}{\xi^*}\varepsilon_y^{nom} E_{yp}\left\{1-\exp(-\xi^*(\varepsilon_u^{nom}-\varepsilon_{yp}^{nom})/\varepsilon_y^{nom})\right\}+\sigma_y^{nom} \tag{3-2}$$

To formulate the uniaxial stress-strain relation, plastic modulus at the beginning of the plastic hardening E_{st}, plastic strain at the end of yield plateau ε_{yp}^{nom}, ultimate tensile strain ε_u^{nom} are the necessary parameters. Regarding the determination of E_{st} and ε_{yp}^{nom}, an average value obtained from tensile coupon test for SS400 $E_{st}/E_s = 1/40$ and $\varepsilon_u^{nom} = 0.237$ is used, while ε_{yp}^{nom} is determined from tensile coupon test results carried for used for circular hollow column No.8 (Public works research institute, 1997-2000). The relation between σ^{nom} and ε^{nom} calculated by using Eq.(3-1) is converted into true stress σ^{true} and logarithmic plastic strain ε_p as follows

$$\sigma^{true} = \sigma^{nom}(1+\varepsilon^{nom}) \tag{3-3a}$$

$$\varepsilon_p = \ln(1+\varepsilon^{nom}) - \frac{\sigma^{true}}{E_s} \tag{3-3b}$$

The computed uniaxial true stress-logarithmic plastic strain relations for material steel are illustrated in **Fig. 3-3**. Considering the relation shown in **Fig. 3-3**, a multi-linear approximation is used to compute the hardening modulus H_m^p and curve fitting parameter ξ for 3-surface model. The remaining cyclic parameters for 3-surface model are f_b/σ_y, β, ρ, and κ. These parameters except f_b/σ_y can be treated as independent of steel grade and taken as standard numerical value (Goto et. al, 2006) for hollow circular columns. Generally, the parameter f_b/σ_y can be determined from the results of cyclic loading test on steel material. In this study, due to lack of cyclic loading test results, this parameter is calibrated by using the unidirectional cyclic loading test results on hollow column (No.29). The results of the specimen No.29 computed from nonlinear FEM shell analysis is expressed in **Fig. 3-4** in terms of horizontal load-displacement relation and compared with the results obtained from cyclic loading experiment. It represents that the computed numerical results best fit with experimental results and the accuracy is confirmed with considering the minimum error optimization technique. Therefore, the computed as well as calibrated all steel material parameters for 3-surface model are summarized in **Table 3-3**.

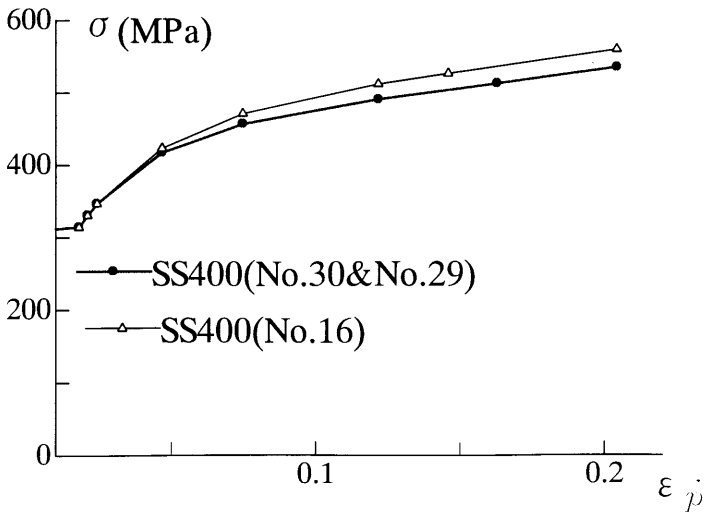

Fig. 3-3 Uniaxial true stress-logarithmic plastic relation for steel

Table 3-3 3-surface model parameters

No.16	No.29&30
E_s = 205.8(GPa)	E_s = 205.8(GPa)
σ_y = 308(MPa)	σ_y = 308(MPa)
σ_u = 559.5(MPa)	σ_u = 534(MPa)
ν_s = 0.3	ν_s = 0.3
ε_{yp} = 0.0183	ε_{yp} = 0.0183
f_b / σ_y = 0.25	f_b / σ_y = 0.25
β = 150	β = 150
ρ = 2.0	ρ = 2.0
κ = 2.0	κ = 2.0
ξ = 0.25	ξ = 0.10
H_m^p(*)	H_m^p(*)

(*) Multilinear curve is used to approximate the hardening behavior (**Fig. 3-3**)

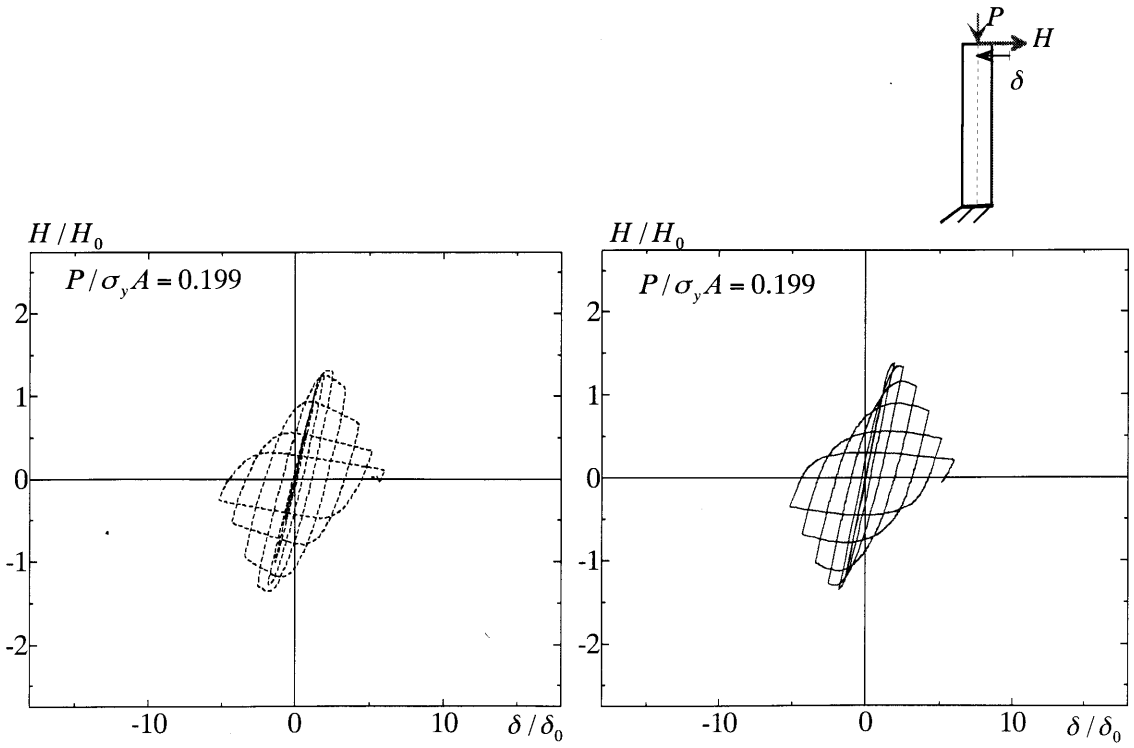

(a) Experiment (b) Analysis

Fig. 3-4 Hollow column specimen (No.29)

3.3.3 In-filled concrete material constants determination

To express the nonlinear behavior of in-filled concrete, concrete damaged plasticity model is used. Some concrete material constants are necessary to define the concrete model, which is categorized into following 5 items.

① Young's modulus E_c and Poisson's ratio ν_c
② Uniaxial stress-strain relation for compression
③ Uniaxial stress-strain relation for tension
④ Damage parameter and equivalent plastic strain relation
⑤ Magnitude of material parameters ψ, e, σ_{b0}/σ_{c0}, K_c

Concerning these five items, it is necessary to compute compressive strength of concrete $f_c^{'}$ obtained from uniaxial compression test on cylinder specimen.

Regarding ①, Young's modulus E_c calculated by following ACI guideline (ACI,1999) $E_c = 4700\sqrt{f_c^{/}}$ MPa and Poisson's ratio $\nu_c = 0.2$ are used to define elastic properties of plain concrete.

Regarding ②, the uniaxial stress-strain curves shown in **Fig. 3-5(a)** is used to define compressive behavior of concrete. The shape of these curves is determined considering the compressive strength of concrete such that the shape is almost proportional to the stress-strain curve shown by Sakino et al. (2004).

Regarding ③, tensile strength of concrete is calculated from 10% compressive strength, $\sigma_{t0} = f_c^{/}/10$ (Matsumura et. al, 2007). To define the tension softening behavior of plain concrete, there is a standard specification proposed by JSCE (2002). This tension softening behavior provides convergence problem when concrete is subjected to larger inelastic deformation. To ensure better numerical stability, the linear stress-crack opening relationship with the negative stiffness graphically shown in **Fig. 3-5(b)** is considered in the post-peak range. This tension softening behavior is dependent on size of the element, which can be calculated from element characteristics length.

In the FEM analysis of PCFT columns, discrete crack model is considered to simulate the cracking behavior of concrete and this discrete crack is located where concrete is subjected to large inelastic deformation. The cracking behavior is simulated with contact pair model and tensile stress becomes zero while tensile force acts on the respective surfaces. Therefore, tension softening behavior with negative stiffness shown in **Fig. 3-5(b)** has no significant effect on overall behavior of PCFT columns.

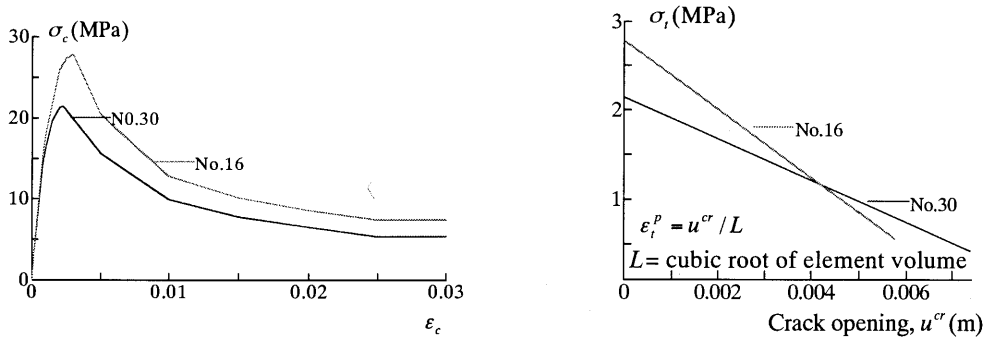

(a) Compressive behavior (b) Tensile behavior

Fig. 3-5 Uniaxial stress-strain relation of in-filled concrete

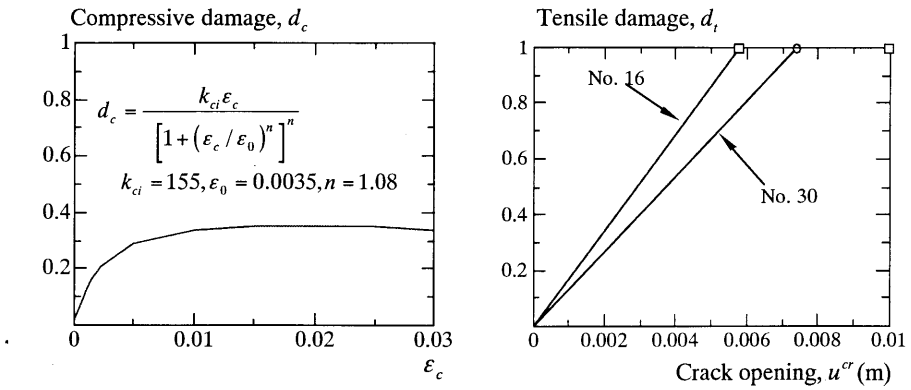

(a) Compressive damage (b) Tensile damage

Fig. 3-6 Damage parameter-strain relation for in-filled concrete

Table 3-4 Damaged plasticity model parameters

Specimen	E_c(GPa)	ν_c	ψ	K_c	σ_{bo}/σ_{co}	e
No.30	21.8	0.2	38°	0.70	1.10	0.2
No.16	24.8					

Regarding ④, the damage parameter of concrete significantly influences the unloading stiffness and size of yield surface. There are specific guidelines recommended by JSCE (2002) to calculate the compressive damage parameter for concrete. However, this guideline provides relatively higher damage even at small inelastic deformation of concrete. As is well known the in-filled concrete is not severely damaged under in-put earthquake waves. That's why for this study, an alternative approach is followed to determine the compressive damage parameter. The relation between damage parameter and compressive strain of concrete shown in **Fig.3-6(a)** is calibrated by using the experimental results of specimen No.30 and 16. The validity of the calibrated compressive damage parameter is confirmed by comparing the computed results with the results of experiments. Specially, the computed hysteretic behavior of PCFT columns better coincides well when unloading occurs. The tensile damage parameters shown in **Fig.3-6(b)** is determined based on ensuring the better convergence for numerical analysis.

Regarding ⑤, The concrete material parameters ψ, e, σ_{b0}/σ_{c0}, K_c can be determined directly from 3-D loading test on concrete specimen. But, there is no available experimental data to compute these concrete material constants. Therefore, following the guidelines recommended by ABAQUS, the three parameters , $\sigma_{b0}/\sigma_{c0}=1.1, K_c=0.7$, $\varepsilon=0.2$ are used to define constitutive relation of concrete. And remaining parameter $\psi=38^0$ is calibrated by using the test results of specimens No.30 and 16 such that the computed results best fit with experimental results. The concrete material constants used for numerical analysis of PCFT columns are summarized in **Table 3-4**.

Furthermore, the 「Elastic in-filled concrete model」 is an approximate model, where in-filled concrete is assumed to be an elastic body that does go into inelastic deformation. The similar elastic properties of concrete E_c and ν_c considered in 「Proposed model」 of PCFT columns will be used for 「Elastic in-filled concrete model」 .

3.3.4 Location of discrete crack surface in in-filled concrete

An alternative to the tensile cracking model used in concrete damaged plasticity model is the introduction of discrete crack surface. This is normally done by disconnecting the displacement at nodal points and interaction between two disconnecting surfaces is modeled by surface based interaction. One obvious difficulty in such an approach is that the location and orientation of the cracks are not known in advance. In this study, discrete crack location is determined by two different ways and schematically shown in **Fig.3-7**.

In 「Accurate model」, discrete crack surface is introduced in in-filled concrete in the position where relatively larger local deformation in horizontal direction occurs. This crack location is associated with the location of local buckling of steel tubular column shown in **Fig. 3-7(a)** (Iura et al. 2002, Morishita et al. 2000). Initially to determine the crack location, it is necessary to compute a FEM analysis without any discrete crack in in-filled concrete and observe the possible location of maximum tensile plastic strain. Then, crack surfaces will be discretized in these possible locations. This approach directly resembles with beam model.

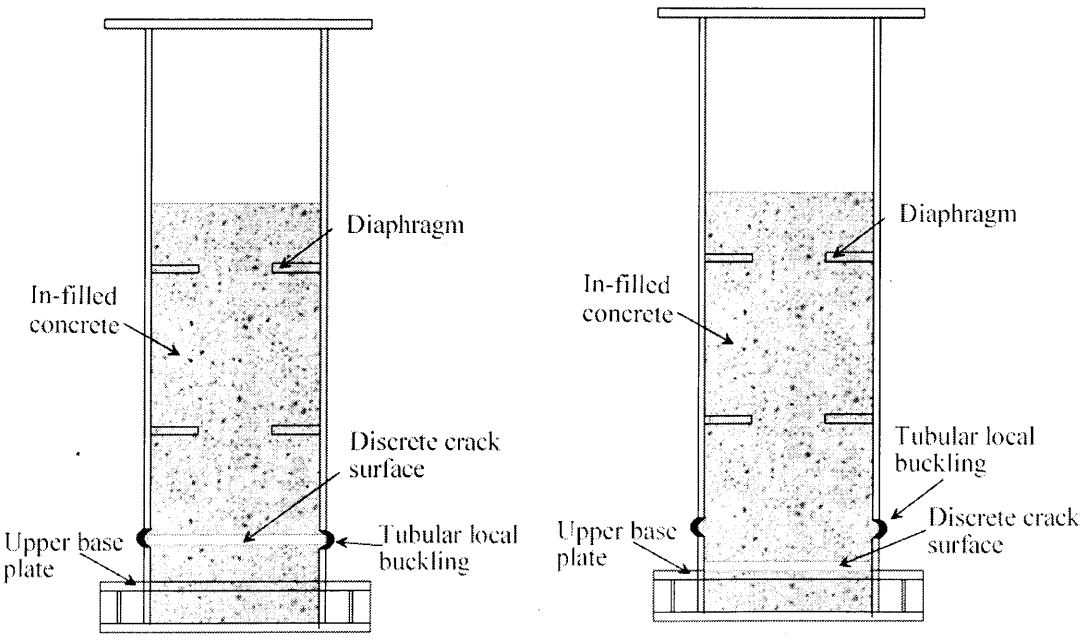

(a) Accurate model (b) Proposed model

Fig. 3-7 Location of discrete crack surface in in-filled concrete

In 「Proposed model」, discrete crack surface is located between below the concrete base and above the upper base plate (**Fig. 3-7(b)**). The basis of this assumption is that when tensile force acts in in-filled concrete, the concrete below upper base plate acts as a rigid body and does not resist concrete above upper base plate to move in vertical direction. Under this situation, there is a possibility to generate discrete crack surface just above the upper base plate. For both cases, the discrete concrete modeling is defined by contact pair and Coulomb friction model, where the co-efficient of friction μ =1.0 (ACI Code Issues) is considered for friction behavior between concrete on concrete surface.

3.3.5 Constants for interface modeling between steel tube and in-filled concrete

The contact behavior between steel-concrete interface is simulated by contact pair model and friction behavior is modeled with Coulomb friction model, which is expressed in Eq.(2-12). As a coefficient of friction between tubular column and in-filled concrete, μ =0.2 (Johansson et al. 2001) is used for FEM analysis.

On the other hand, to investigate the interface modeling effect, the contact pair with Coulomb friction model is replaced by the contact with shear spring model. In the spring model, three spring constants are used to express contact and friction behavior, such as k_r, k_z,k_θ. In this study, bi-linear spring model is used to express contact behavior, where, $k_r = 9.8\times10^9$ KPa/cm (Fujii et al. 2003) is used for compression side, while $k_r = 0.0$ is considered for tension side. And linear shear spring is used in two orthogonal directions. To define the shear spring model, $k_z = k_\theta = 2764$ KPa/cm (Charles et al. 1999) is used for numerical analysis.

3.4 Comparison the hysteretic behaviors of PCFT columns computed from different FEM models

The results of unidirectional cyclic loading tests on PCFT (No.30&No.16) columns are compared with the results computed from 4 types of FEM models in terms of the horizontal restoring force-displacement relation.

a) Proposed model

In **Fig.3-8** &**3-9**, the computed results of the 「Proposed model」 are compared with the results of experiments on PCFT columns (No.30 & No.16). The accuracy of the FEM model is generally acceptable. Specifically, the computed results rather

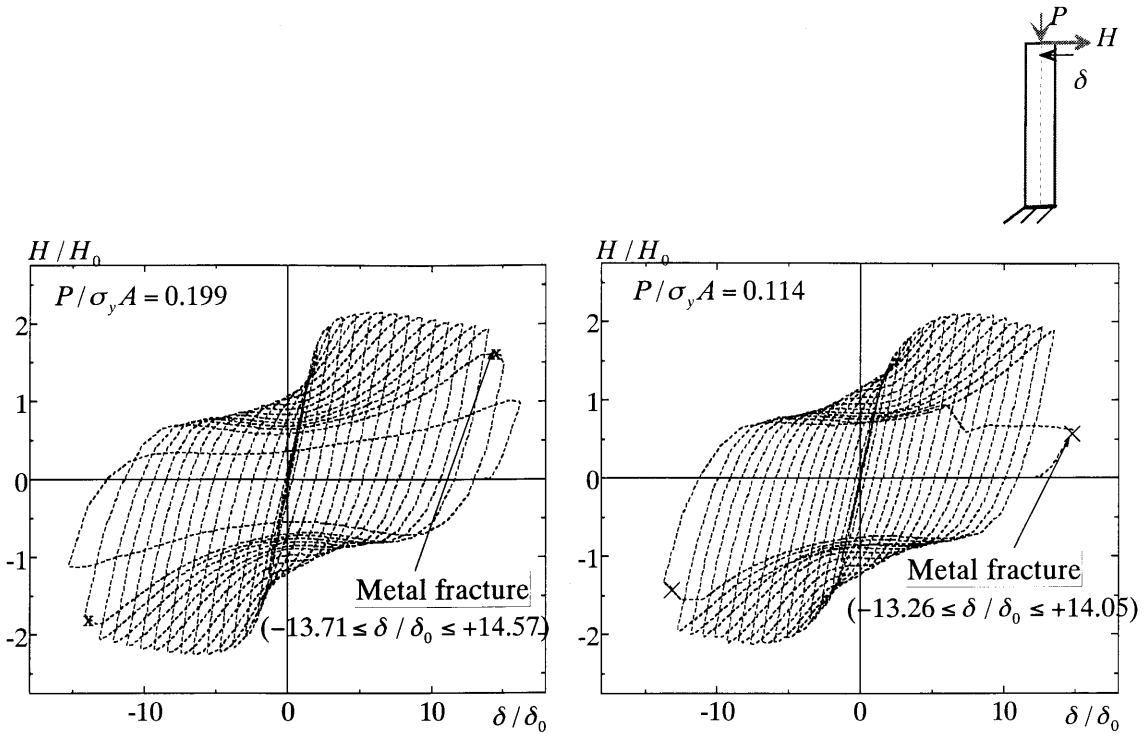

(a) No.30 (b) No.16

Fig. 3-8 Experiment

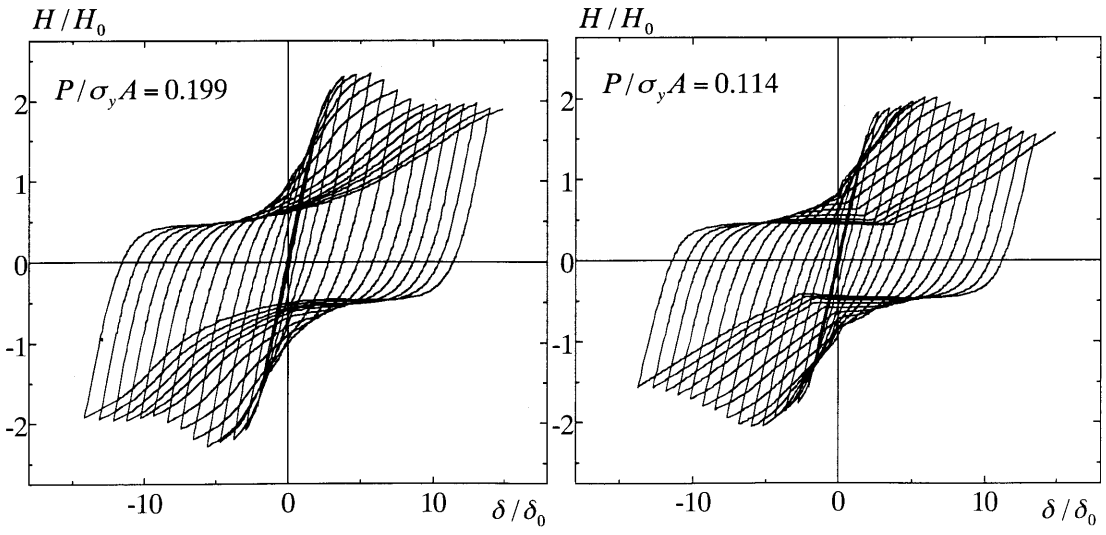

(a) No.30 (b) No.16

Fig. 3-9 Proposed model

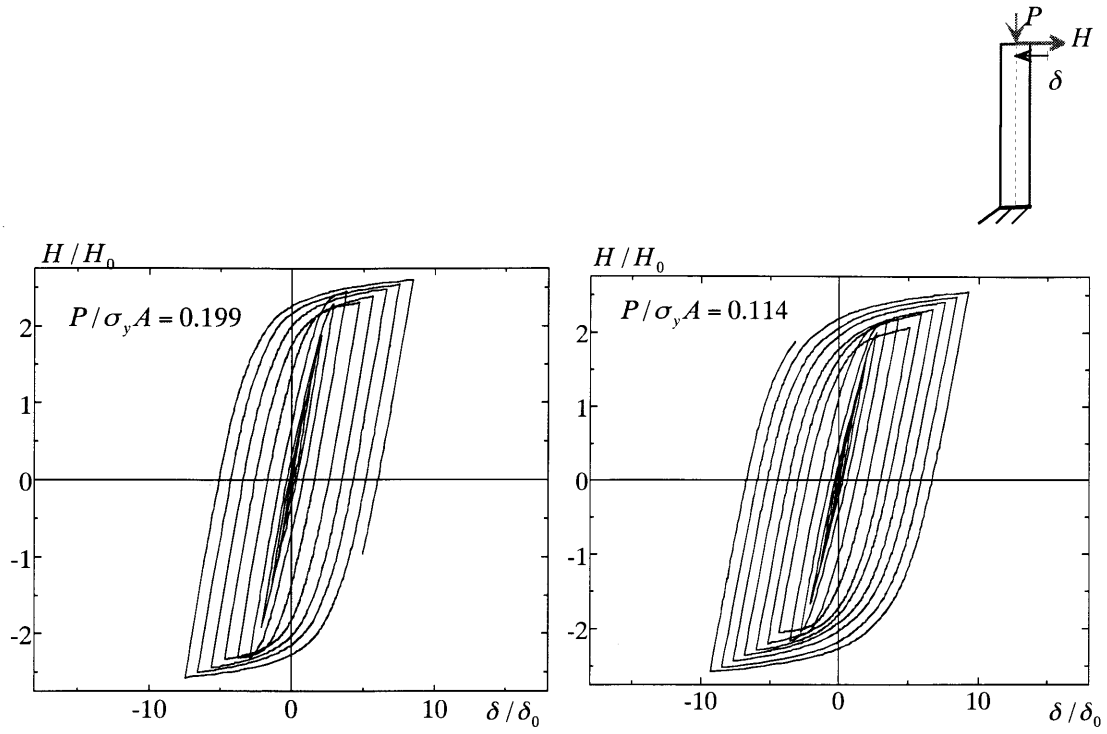

(a) No.30 (b) No.16

Fig. 3-10 Proposed model without any discrete crack surface

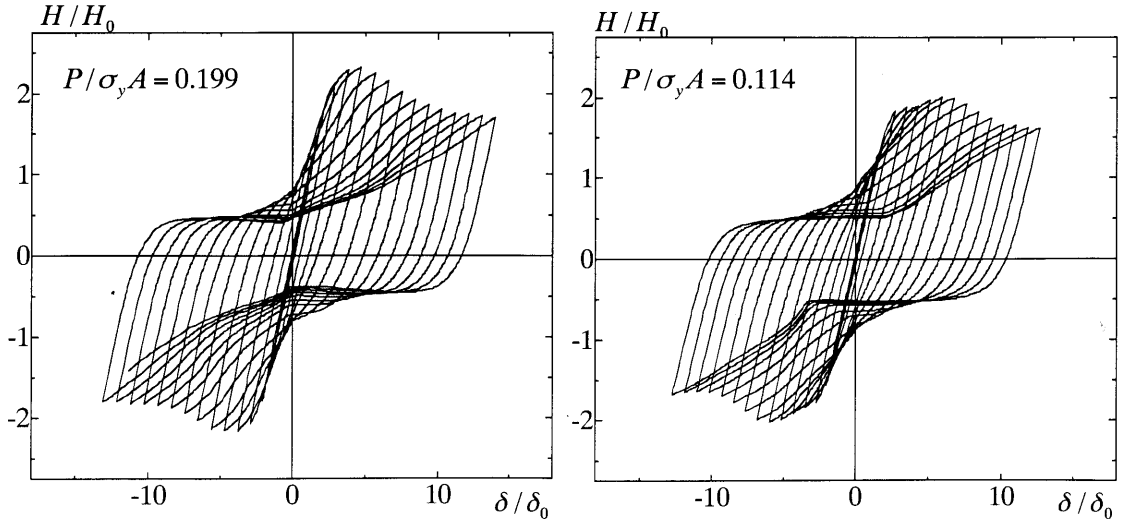

(a) No.30 (b) No.16

Fig. 3-11 Accurate model

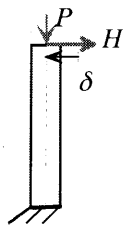

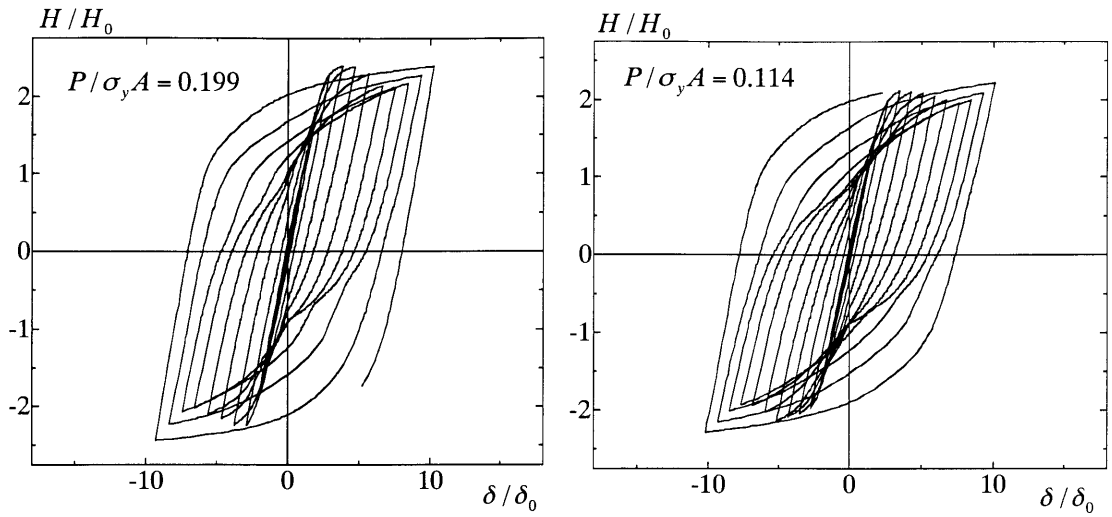

(a) No.30 (b) No.16

Fig. 3-12 Boundary spring model

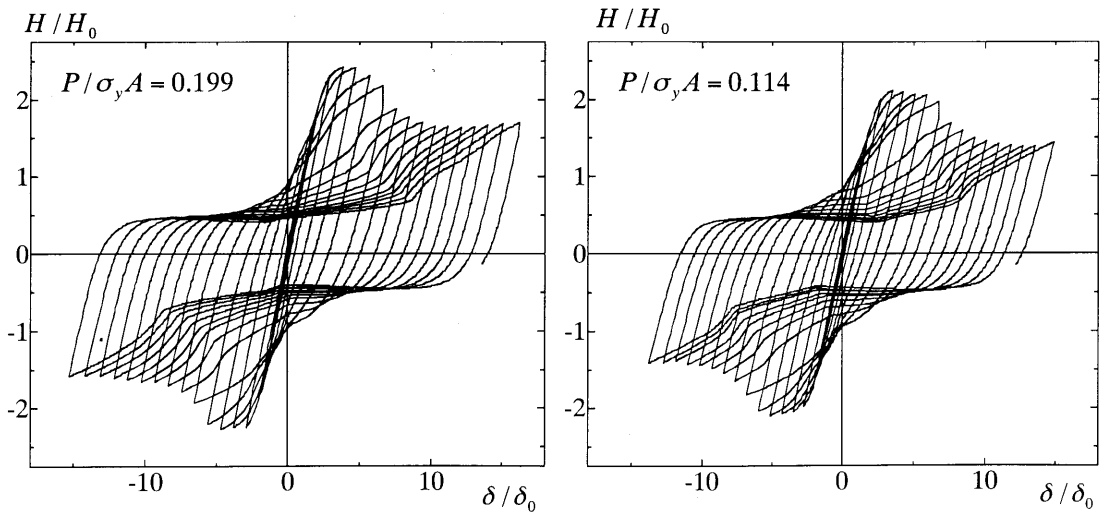

(a) No.30 (b) No.16

Fig. 3-13 Boundary spring model with removal of spring from buckling area

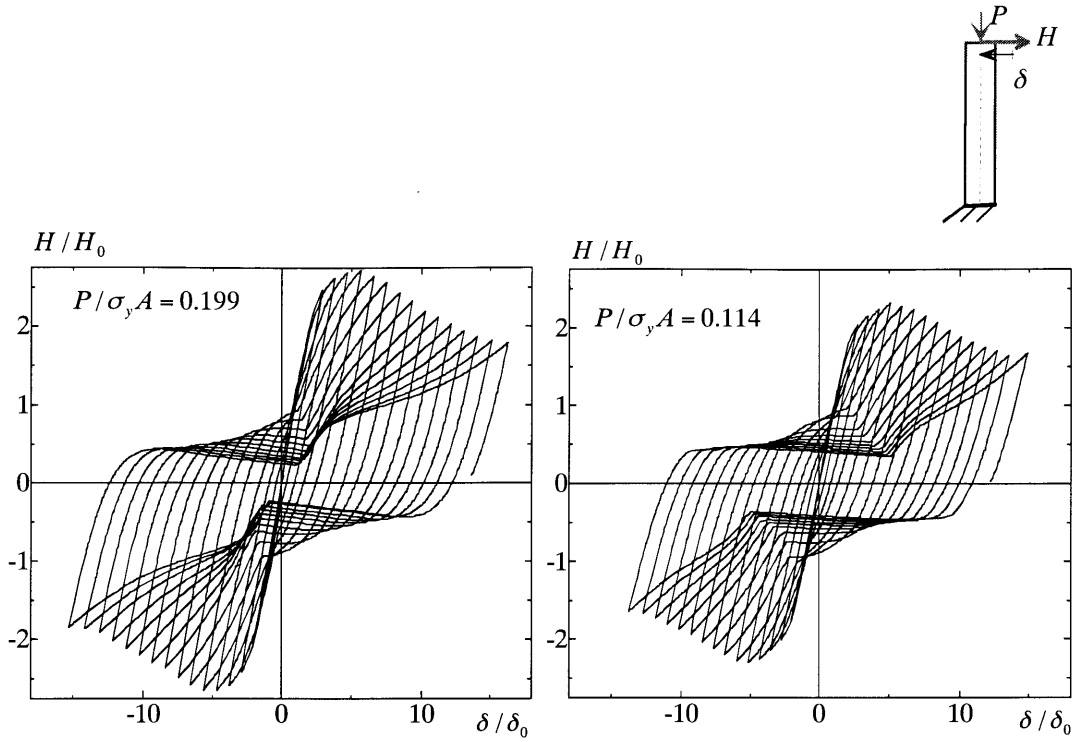

(a) No.30 (b) No.16

Fig. 3-14 Elastic in-filled concrete model

accurately exhibit the pinching hysteretic loops observed in the experiments of PCFT columns. In the post peak range, computed softening behavior differs from the results of experiments a little bit. This is due to metal fracture occurred in steel tube at outer surface. After first occurrence of metal fracture at steel tube, the structural behavior will change drastically. Therefore, it is very difficult to compute this drastic change in softening behavior numerically.

The computed results of the 「Proposed model」 with considering no discrete crack surface introduced in in-filled concrete are shown in **Fig.3-10**. It represents that the computed results differ completely and pinching hysteretic loop characteristics observed in the experiments, disappears both in pre-peak and post-peak range. This because the damaged plasticity model cannot predict the cyclic crack opening and crack closing in filled concrete more accurately.

b) Accurate model

The objective of this model is to investigate the effect if the position of discrete crack is changed the location of crack surface above the upper base plate. In this

model, the crack location that is used to construct「Proposed model」, is changed and relocated at the position where local buckling deformation of tubular columns occurs. The localization occurred at steel tube of specimen No.30 & No.16 is at a distance of $0.11D$ from the upper base plate. The computed hysteretic behaviors of PCFT columns are shown in **Fig.3-11** and compared with the experimental results expressed in **Fig.3-8**. It represents that the computed results also show pinching hysteretic loop characteristics and stiffness of pinching hysteretic curves does not differ significantly comparing with the results obtained from 「Proposed model」. This is because position of the horizontal discrete crack surface in in-filled concrete is very close to the upper base plate and there is no significant change in cyclic crack opening and crack closing pattern observed in 「Proposed model」.

c) Boundary spring model

The objective of this model is to investigate the effect if the interaction model between tubular column and in-filled concrete is changed from the interface model used in 「Proposed model」. In this case, spring model is used as interface model, which resembles with contact pair and Coulomb friction model and considers the contact with friction behavior along the interface between steel tube and in-filled concrete. The computed hysteretic behaviors are shown in **Fig.3-12**. Comparing with experimental results (**Fig.3-8**), it is clear that the computed hysteretic behaviors using spring model coincide well with the results of experiments up to $6\delta_0$ displacement amplitude. While local buckling deformation becomes large, the change in computed pinching hysteretic loop characteristics is remarkable at a displacement amplitude of $7\delta_0$, comparing with experimental results. This is because the orientation of the steel-concrete interface changes drastically, while local buckling deformation occurs at steel tube.

In「Boundary spring model」, linear shear spring is inserted at the interface of tubular column and in-filled concrete in horizontal and vertical directions. Beyond $7\delta_0$ displacement amplitude, the shear springs inserted in tubular buckling area (at a distance of $0.025D \sim 0.15D$ from upper base plate) have been removed, and the computed results after removal of these shear springs are shown in **Fig. 3-13**. It represents that computed results with removal of shear spring from tubular buckling area show relatively stable pinching hysteretic loop characteristics. However, as expressed above, sudden removal of spring makes the numerical calculation more

difficult. It is fact that equivalent nodal forces are removed abruptly and thereby, external force acting at the spring elements is enforced to backwards. This phenomenon indirectly influences the slope of descending envelops of hysteretic curves. The removal of spring will be considered as a special algorithm to compute the hysteretic behavior of PCFT columns, if springs are used as an interface element.

d) Elastic in-filled concrete model

A relatively simplified and approximate model to compute the hysteretic behavior of PCFT columns is to consider the in-filled concrete as an elastic body and ignore the concrete damaged plasticity. This model resembles with 「Proposed model」 in the sense that discrete crack surface is located near upper base plate. The computed hysteretic behaviors shown in **Fig.3-14** exhibit well agreement with 「Proposed model」 comparing the pinching hysteretic loop characteristics of PCFT columns. But the computed horizontal restoring force is significantly increased up to displacement amplitude of $6\delta_0 \sim 7\delta_0$. This is because no damaged plasticity in concrete is taken into consideration. This model can also ensure that the crack opening and crack closing occurs cyclically at the discrete crack surface. Therefore, with compromising the nonlinear behavior of in-filled concrete, it is possible to obtain a more simplified hysteretic model for PCFT columns.

3.5 Failure mechanism of PCFT columns under cyclic loading

The failure mechanism of PCFT columns comprises of localized deformation in steel tube, increasing the compressive strength of in-filled concrete due to confining pressure effect, and occurrence of fracture in steel tube due to large equivalent strain localization. Herein, to describe the failure mechanism, the results of experiment (public works research institute, 1997-2000) on PCFT columns (No.30) under unidirectional cyclic load is considered and computed results based on proposed FEM model are added to clarify the failure mechanism details.

3.5.1 In-filled concrete restraining effect on tubular local buckling

To investigate the in-filled concrete effect, the computed deformed shapes at lower part of steel tubes of PCFT (No.30) and corresponding hollow (No.29) columns shown in **Fig.3-15(a) & (b)** are compared at the same displacement amplitude. The

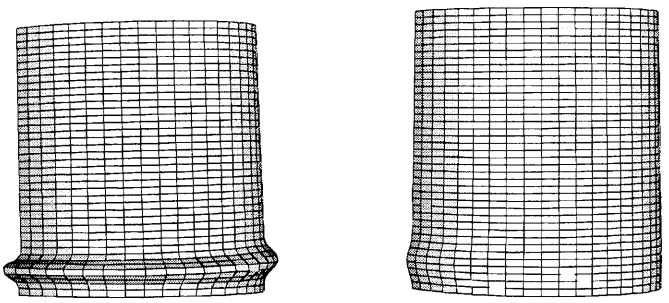

at $\delta = +6.0\delta_0 = 63$mm

(a)Hollow (No. 29) (b) PCF (No.30)

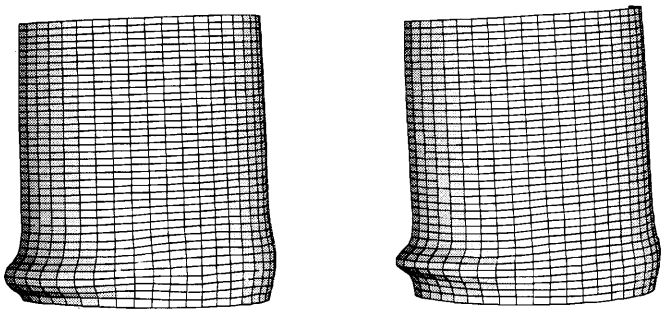

at $\delta = +13.33\delta_0 = 140$mm at $\delta = +12.14\delta_0 = 140$mm

(c) PCFT (No. 30) (d) PCFT (No.16)

Fig. 3-15 Deformed shape at the lower part of steel pipes (× 1.5)

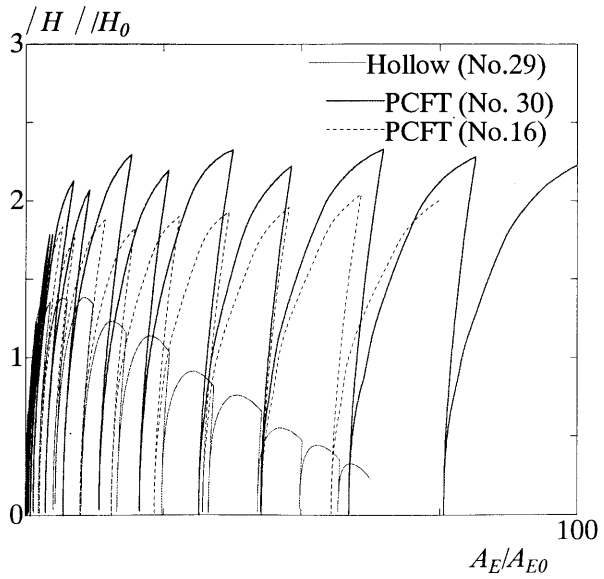

Fig. 3-16 Dissipated energy-absolute horizontal restoring force relation up to $\delta = +6.0\delta_0$

comparison of deformed shapes of steel columns represents that no significant inelastic local deformation occurs in PCFT column, while the hollow column goes to large inelastic local deformation that develops along loading direction near column base. This buckling patterns observed in outer shell are similar to elephant foot buckling modes, which changes cyclically with loading direction. The inward local buckling of PCFT column is delayed by in-filled concrete restraining effect. This is due to dilation of in-filled concrete near to the tubular buckling area and cyclic interaction between the interfaces of steel tube and in-filled concrete.

To investigate the effect of axial stress ratio on local deformation, the deformed shapes of PCFT column specimens (No.30 & No.16) are compared (**Fig.3-15(c) & (d)**) at the same displacement amplitude. Herein, the PCFT (No.30) column is subjected to higher axial stress ratio comparing with No.16. The comparison implies that the PCFT specimen subjected to higher axial stress ratio exhibits larger inelastic local deformation.

Furthermore, to examine the effect of the in-filled concrete, the dissipated energy-horizontal restoring force relations are further shown for PCFT and hollow columns in **Fig. 3-16**. In **Fig.3-16**, the plastic energy dissipated by the column is approximately calculated by $A_E = \int H d\delta$ and A_{E0} is an elastic energy given by $A_{E0} = 0.5 H_0 \delta_0$. From **Figs.3-4, 3-9, 3-15 & 3-16,** the strength, ductility and energy dissipation capacity of PCFT columns are significantly improved from those of the hollow columns. This is primarily due to fact that the local buckling of the steel tube is restrained by the in-filled concrete (**Fig.3-15**).

3.5.2 Axial stress and confining pressure distribution on in-filled concrete

To investigate the confining pressure effect on in-filled concrete strength, bottom layer of concrete near base plate is taken into consideration. The bottom layered concrete is divided into tensile and compressive zone when it is subjected to bending action. These two zones are separated from each other in a criterion of axial stress is either tensile or compressive. This zone distinction derived from the results of FEM analysis of PCFT column (No.30) is shown in **Fig. 3-17**. It represents that tensile crack opening/crack closing occurs periodically with changing the loading direction, which is significant for developing the typical hysteretic curve of PCFT columns. Under the compressive zone, the compressive stress acting on bottom layered concrete is gradually increased to maximum $1.72 f_c'$ at $\delta = +12.16\delta_0$ This can be explained that

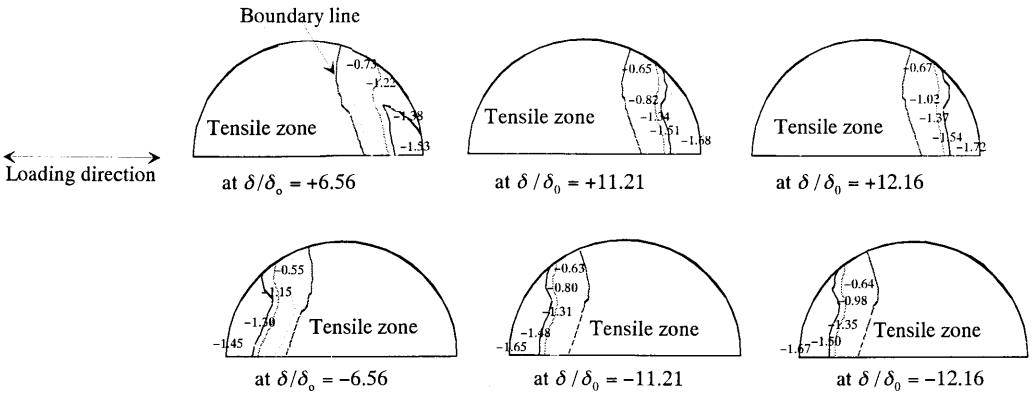

Fig. 3-17 Axial stress distribution on in-filled concrete element above upper base plate of the specimen No.30 (axial stress/ f_c')

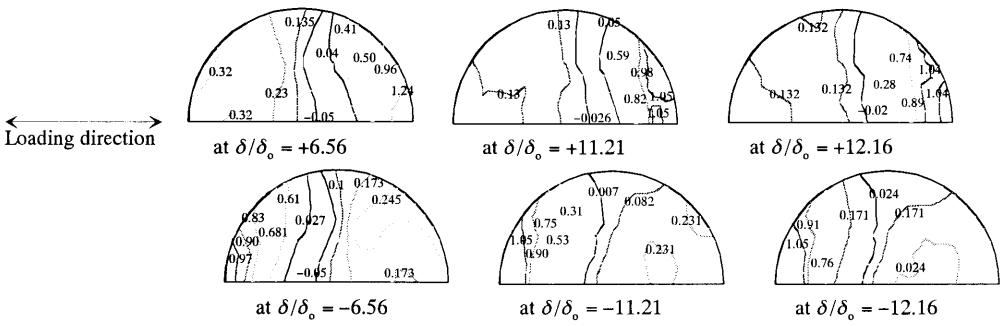

Fig. 3-18 Confining pressure distribution on in-filled concrete element above upper base plate of the specimen No.30 ($(\sigma_m / f_c' = -(\sigma_{xx} + \sigma_{yy} + \sigma_{zz})/3f_c')$)

internal passive pressure results from steel tube acts as confinement to the in-filled concrete and increases the strength of concrete.

It is of interest to investigate either the concrete filled in steel tube is subjected to high confining pressure or not. In a PCFT column, compressive confining stresses on the concrete core are induced by passive confinement provided by the outer steel tube. The circular steel tube has a high stiffness against inner pressure perpendicular to the tube wall, and therefore circumferential steel hoop tension can develop to provide lateral confining pressure to the concrete core. Due to this lateral confinement, concrete behaves like a ductile material. The concrete damaged plasticity model can effectively evaluate this confining pressure in multiaxial stress state. To examine this pressure distribution on in-filled concrete, bottom layered concrete for PCFT column (No.30) is taken into consideration, where relatively larger local deformation occurs. The confining pressure distributions are shown in **Fig.3-18** in terms of contour lines. From this pressure distribution, it is clear that the concrete elements adjacent to the steel tube suffer from maximum confining pressure up to $1.04 f_c'$ at a displacement of $\delta/\delta_0 = +12.16$. It is clear that increment of maximum confining pressure acting on concrete element satisfies well the allowable limit (4 to 5 times f_c'), recommended by concrete damaged plasticity model.

3.5.2 Strain localization and metal fracture occurrence at local buckling of steel tube

The outer shell of PCFT column is likely to go into relatively larger inelastic deformation, compared with hollow column. As a result, metal fracture is likely to occur due to high strain localization developed in outer steel tube. Basically, the crack initiation is ductile fracture in nature. In this study, metal fracture initiation criterion is investigated based on equivalent plastic strain localized in buckling of steel tube. During the cyclic loading experiments on PCFT columns (No.30), metal fracture is observed on the outer surface at amplitude of $\delta = +14.57\delta_0$. The location of metal fracture along with tubular local buckling is located at 100 mm above the base plate, which is schematically shown in **Fig.3-19**. A relation between equivalent plastic stain and horizontal displacement acting on top of the column is computed from the results of FEM analysis for PCFT and corresponding hollow columns. The computed results are shown in **Fig.3-20** for comparison. It represents that the fracture first initiates from outer surface when equivalent plastic strain $\bar{\varepsilon}^p = 1.21$ at amplitude of $-13.71\delta_0$, Moreover, hollow column is far from fracture initiation problem. So, this key feature should be taken into consideration for practical design of PCFT column, even though it is very effective for earthquake resistance.

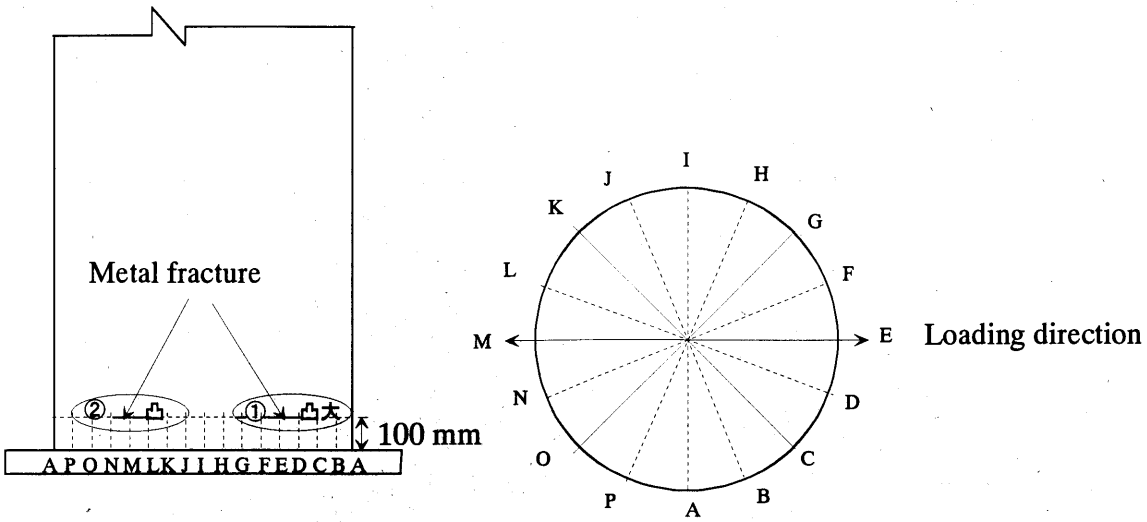

Fig. 3-19 Fracture location at steel tube (No.30)

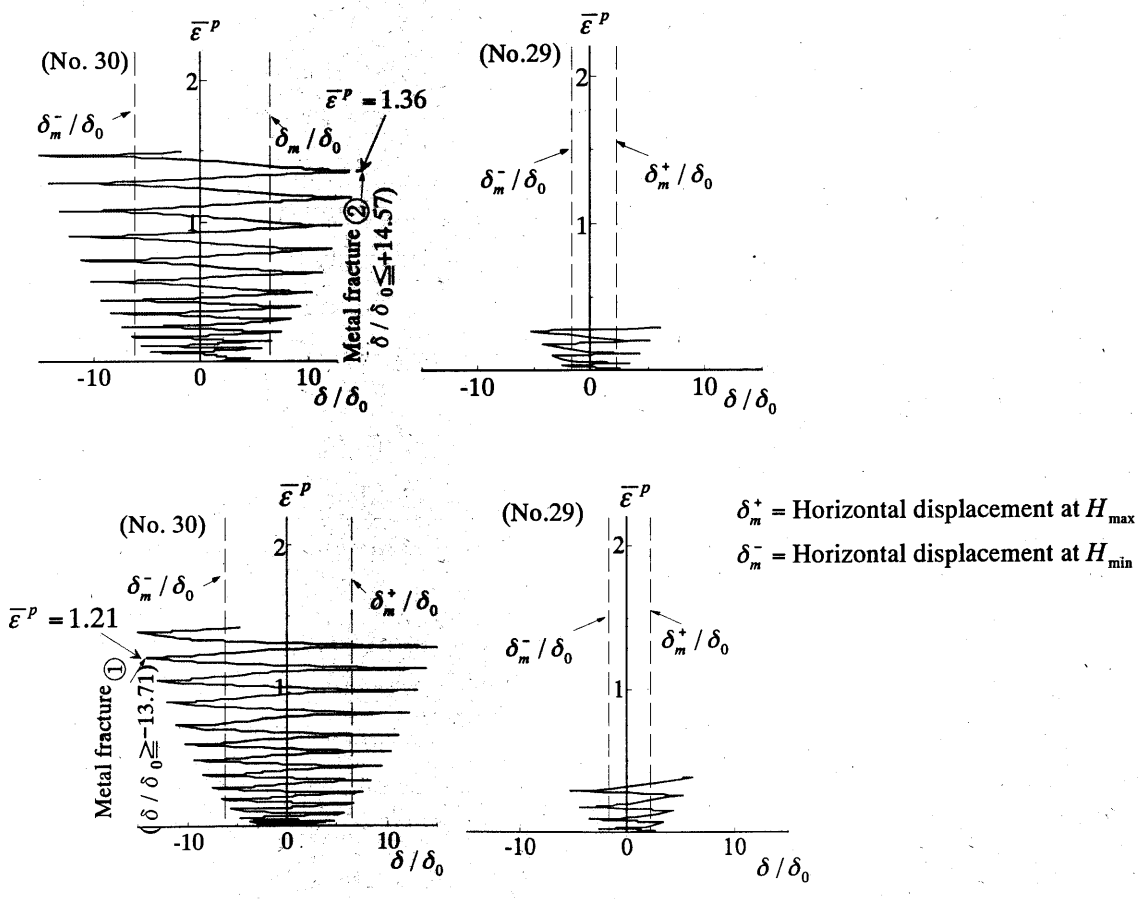

Fig. 3-20 Fracture occurrence at outer surface of steel tube with change of equivalent plastic strain

3.6 Summary and Concluding Remarks

This chapter outlines a 3D FEM model that computes the hysteretic behavior of PCFT columns under unidirectional cyclic load. In this model, steel tube is modeled by nonlinear geometric 4-node thick shell element with local buckling and the material nonlinearity is expressed by 3-surface cyclic plasticity model, while in-filled concrete is represented by 8-node solid element and concrete nonlinear behavior is defined by damaged plasticity model. The interaction between tubular column and in-filled concrete is simulated with contact pair with Coulomb friction model. Herein, the results obtained from a stable and accurate FEM model is presented in comparing with experimental results. From this computation, following conclusions can be drawn.

(1) In 「Proposed model」, discrete crack surface is introduced between upper base plate and bottom part of in-filled concrete. This model represents an accurate and stable FEM model to compute the hysteretic behavior of PCFT columns that exhibits the pinching hysteretic loop characteristics observed from experiments.

(2) 「Accurate model」 is an alternative way of 「Proposed model」 where discrete crack surface is replaced in in-filled concrete, where steel tube goes into larger inelastic deformation. The computed results do not differ significantly in comparing with the results of 「Proposed model」. This is because location of local buckling deformation is very close to the upper base plate.

(3) The computed results from 「Proposed model」 with no discrete crack surface in in-filled concrete differs significantly comparing with results of experiments. This is because tensile behavior of in-filled concrete defined by damaged plasticity model can not predict cyclic crack opening and crack closing accurately.

(4) The results obtained from 「Boundary spring model」 also show pinching behavior up to ultimate state. But in post-peak range, when local buckling bulge forms in tubular columns, steel tube goes into larger inelastic deformation and spring orientation is altered abruptly, which greatly influences the hysteretic behavior of PCFT columns. These problems can be minimized by removing the spring elements at a time when localization initiates in steel tube. Hence a special algorithm will be considered to remove the spring elements from tubular buckling zone.

(5) The 「Elastic in-filled concrete model」 is similar to 「Proposed model」, but differs in ignoring the concrete inelasticity. The basis of this model is that the concrete

filled at lower part of steel column is confined by diaphragm and not seriously damaged during earthquake. This results in increasing the ultimate strength capacity of PCFT columns. But in post peak range, no significant difference is observed comparing with experimental results.

(6) Based on 「Proposed model」, concrete material parameters are calibrated. At the same time, the axial stress and confining pressure distribution on in-filled concrete layer close to upper base plate are investigated, which represents that strength of in-filled concrete increases due to confining pressure provided from steel tube. In addition, local buckling of steel tube is restrained due to concrete dilation and steel-concrete interaction. Thereby, the strength and deformation capacity of PCFT columns are significantly improved, comparing with hollow tubular columns.

(7) The PCFT columns are subjected to large inelastic deformation. Therefore, steel tube suffers from larger equivalent plastic strain, which results in fracture initiation in steel tube. So, the occurrence of metal fracture must be considered for practical design of PCFT columns.

Chapter 4

Summary

4.1 Summary and concluding remarks

The work presented in this thesis is a study of hysteretic behavior of thin-walled steel tubular column with partially in-filled concrete. In this study, 4 types of 3-D FEM models for PCFT columns are determined based on discrete crack location in in-filled concrete, an accurate as well as relatively approximate model for interaction between tubular column and in-filled concrete, and constitutive model used for in-filled concrete. The objective of constructing FEM models is to investigate the hysteretic behavior of PCFT columns under unidirectional cyclic load. The observations based on numerical computation are primarily concentrated on deriving the typical hysteretic loop characteristics that observed in the unidirectional cyclic loading experiments on PCFT columns. The numerical analysis is carried out by using general-purpose FEM package program ABAQUS ver. 6.6, in which 3-surface cyclic plasticity model for steel and concrete damaged plasticity model for in-filled concrete are used as constitutive relation. In this analysis, steel tube and in-filled concrete are represented by nonlinear shell and solid elements, respectively. Contact pair along with Coulomb friction model, and spring model are used to simulate steel-concrete interaction. The overall findings from this analytical study are summarized below.

(1) A more accurate and numerically stable FEM model, referred hereinafter as 「Proposed model」 is presented to compute the hysteretic behavior of PCFT column under cyclic unidirectional load. In comparison with experimental results, the accuracy of the computed hysteretic behavior of PCFT column is proved to be generally acceptable. Specifically, the computed results exhibit the pinching hysteretic loops that observed in the unidirectional cyclic loading experiments of PCFT columns.

(2) An 「Accurate model」 is presented for PCFT columns in order to investigate the effect of discrete crack location near local buckling of tubular column. It is observed that the overall hysteretic behavior of PCFT columns does not differ significantly comparing with that of 「Proposed model」 . This is because tubular local buckling occurs at a very close distance to upper base plate.

(3) Comparing with 「Proposed model」, an approximate but numerically stable 「Boundary spring model」 is presented for PCFT columns in order to overcome the contact problem between steel tube and in-filled concrete. Although this model can ensure better convergence, but a special algorithm defined as removal of spring elements from local buckling area, is taken into consideration for post buckling analysis.

(4) An alternative of 「Proposed model」 is referred hereinafter as 「Elastic in-filled concrete model」 is presented for PCFT column. This model ignores the concrete inelasticity assuming that concrete filled at lower part of hollow column is confined by diaphragm and not severely damaged under earthquake waves. Due to this assumption, ultimate strength of PCFT columns is increased a little bit, but post peak results better coincide with experimental results.

(5) Based on 「Proposed model」, it is observed that the cyclic local buckling of thin-walled steel tubular columns is delayed by the interface action and dilation of in-filled concrete. It implies that the strength, ductility and energy dissipation capacity of hollow columns can be significantly improved by the partially in-filled concrete. Therefore, PCFT columns are very effective in order to upgrade the seismic performance of existing thin-walled steel hollow columns.

(6) In PCFT columns, steel tube goes to large inelastic deformation under cyclic load and metal fracture is likely to occur in steel tube due to large inelastic strain localized near local buckling of steel tube. Therefore, this metal fracture initiation criterion should be taken into consideration for practical design of PCFT columns.

4.2 Future research plan

The present analytical study is mainly focused on the computation of ultimate hysteretic behavior of PCFT columns under cyclic unidirectional load. But to ensure the safety of elevated highway bridges under great earthquakes, it is important to predict bi-directional hysteretic behavior of PCFT columns. In context of increasing the seismic resistance of CFT bridge piers, the concept of hysteretic behavior of PCFT columns is to be updated. Therefore, following scopes are recommended for further research.

(1) A 3D FEM model to compute the hysteretic behaviors of thin-walled tubular columns with partially in-filled concrete under horizontal bi-directional cyclic load and the accuracy of the FEM model is to be confirmed by comparing with the results of cyclic bidirectional loading experiments.

(2) An experimental and analytical investigation on hysteretic behavior of PCFT columns under dynamic load.

(3) An extensive investigation on the effects of loading programs on strength and ductility of PCFT columns and determine the best seismic loading program that resembles with earthquake wave.

(4) A design method of PCFT columns that includes optimum height of in-filled concrete as well as design and location of diaphragm over in-filled concrete.

Acknowledgement

The study represents the finite element analysis of hysteretic behavior of thin-walled steel bridge piers with partially in-filled concrete. The research work presented here as a part of Doctor thesis at Nagoya Institute of Technology. First, I would like to express sincere and deepest gratitude towards my academic supervisor **Prof. Yoshiaki Goto** for his consistent guidance, support, valuable discussions, suggestions and continuous encouragements. Under the tireless leadership and unfailing support of **Prof. Goto,** I am able to acquire innovative idea and new knowledge and apply this knowledge in my research work. I greatly acknowledge his endless contribution to this research.

I am greatly indebted to the members of dissertation examining committee, **Prof. Yoshiaki Goto, Prof. Makoto Obata, Prof. Toshikatsu Ichinose, Prof. Zhang Feng** for their valuable discussions, comments, advices and suggestions in reviewing and refining the content of this thesis.

I also express my sincere thanks to all members of structural and earthquake engineering laboratory at Nagoya Institute of Technology for their kind cooperation and assistance during my study and research work, namely Mr. Takemasa Ebisawa and Dr. Naoki Kawanishi.

In particular, I would like to convey my special thanks to all research team members of this laboratory for their helps to remove Japanese language difficulties and making a friendly environment for research. My post graduate study program is financially supported by the Japanese Ministry of Education, Science and Culture through the Monbukagakusho scholarship. To whom I am very grateful and offer the results of my doctoral research as a very humble present.

Finally, I am solely committed to my beloved country Bangladesh to apply tiny knowledge and small power in developing innovative idea and modern technology. Last of all, I express my deepest thanks and gratitude towards my mother and family members for their mental support, encouragement, wish and love, which will be never-ending in my whole life.

REFERENCES

Abdelhafid Bouzaiene and Bruno Massicotte 1997. Hypoelastic tridimensional model for nonproportional loading of plain concrete, J. of eng. mech. div. ASCE, vol.23, no.11, pp.1111-1119.

ACI: Building code requirement for structural concrete and commentary, *ACI318-99*, Detroit, 1999.

ACI Code Issues-Coefficient of friction : concrete to concrete, http ://www.eng-tips.com/viewthread.cfm?qid=11539

Chen, W. F. 1982. Plasticity in reinforced concrete. McGraw-Hill, Inc, USA.

Chen, A.C T., and Chen, W. F. 1975(a). Constitutive Relations for Concrete, J. eng. mech. div. ASCE, vol.101, no. EM4, proc.pap.11529, August, pp.465-481.

Charles W. Roeder, Brad C., and Colin B. Brown 1999. Composite Action in Concrete Filled Tubes, *J. of Struct. Engrg.*, ASCE, 125(5), pp. 477-484.

David Darwin and David A. Pecknold 1977. Nonlinear biaxial stress strain law for concrete, J. Eng. mech. div. ASCE, vol.103, no. EM2, pp.229-241.

Fujii, K., Fujii, T., & Dai, H. 2003. An analysis on concrete filled steel tubular circular column under cyclic horizontal loads. J. of Struct. Engrg., JSCE, Vol. 49A, pp.1041-1050.

Goto, Y., Wang, Q.Y. & Obata, M. 1998. FEM analysis for hysteretic behavior of thin-walled columns. J. Struct. Eng., ASCE, 124(11), pp.1290-1301.

Goto, Y., Jiang, K. & Obata, M. 2006. Stability and Ductility of Thin-Walled Circular Steel Columns under Cyclic bidirectional Loading. J. Struct. Eng., ASCE, 132(10), pp.1621-1631.

Goto Y., and Ghosh P. K. 2007. Hysteretic behavior of thin-walled steel tubular columns with partially in-filled concrete, Proc. of Third International Conference on Steel and Composite Structures (ICSCS07), Manchester, England, pp.813-819.

Goto Y., Ghosh P. K., and Kawanishi N. 2008. FEM analysis for hysteretic behavior of CFT bridge piers considering interaction between steel tube and in-filled concrete, Doboku gakkai ronbunshu (submitted)

Ghosh P. K. and Goto Y. 2008. Stability and ductility of thin-walled steel tubular columns with partially in-filled concrete, Proc. of Fifth International Conference on Thin-walled Structures (ICTWS2008), Brisbane, Australia, pp.983-990.

Hanbin Ge & Usami, T. 1996. Cyclic test of concrete filled steel box columns. J. of structural engineering, ASCE, 122(10), pp.1169-1177.

HKS. 2006 ABAQUS/Standard User's Manual, Version 6.6, Hibbit, Karlson &Sorensen, Inc.

Hsu, H.-L.& Yu, H.-L. 2003. Seismic performance of concretfilled tubes with restrained plastic hinge zones. J. of Construct. Steel Research, 59, pp. 587-608.

Iura, M., Orino, A. & Ishizawa, T. 2002. Elasto-plastic behavior of concrete-filled steel tubular columns. J. Struct. Mech. and Earthquake Engrg., JSCE, No.696/I-58, pp.285-298.

Ishikawa N., Kobayashi Y., Kurihara M., Osawa K., & Toyoda M. 1999 . Ductile Crack Initiation Behavior of Structural Steel under Cyclic Loading, Tetsu-to-Hagane vol. 85, No.1, pp.71-77

Johansson, M. and Gylltoft, K. 2001. Structural behavior of slender circular steel-concrete composite columns under various means of load application, *Steel and Composite Structures*, Vol.1, No.4, pp.393-410.

Japan Road Association 2002. Specification for road bridges and commentaries: V. Seismic design.

JSCE committee on steel structure 1996. Seismic design guiding proposal and new technology for steel, (in Japanese).

JSCE 2002. Standard specifications for concrete structures-2002, seismic performance verification. (in Japanese)

Lee, J., & Fenves, G. L. 1998. Plastic-Damage Model for Cyclic Loading of Concrete Structures. Journal of Engineering Mechanics, ASCE, 124(8), pp.892–900.

Matsumura, T. & Mizuno, E. 2007. 3-D FEM analyses on internal state inside the concrete filled steel tubular columns subjected to flexural deformation under axial loading, J. of Struct. Engrg., JSCE, 53A, pp. 75-83 (in Japanese).

Morishita, M., Aoki, T. & Suzuki, M. 2000. Experimental Study on the Seismic resistance performance of Concrete-filled Steel Tubular Columns. J. of Struct. Engrg., JSCE, 46A, pp.75-83.

Public Work Research Institute. 1997-2000. Report of cooperative research on limit state seismic design for bridge piers I-VIII and summary.

Sakino, K., Nakahara, H., Morino, S. & Nishiyama, I. 2004. Behavior of Centrally Loaded Concrete-Filled Steel-Tube short Columns, J. of Struct. Engrg., ASCE, 130(2), pp.180-188.

Susantha, K. A. S., Hanbin Ge & Usami, T. 2002. Cyclic analysis and capacity prediction of concrete-filled steel box columns. Earthquake Engrg. And Struct. Dynamics, 31, pp.195-216.

Toader A. Balan and Egor P. Popov 1997. Constitutive model for 3-D cyclic analysis of concrete structures, J. of eng. mech. div. ASCE, vol.23 no.2, pp.143-153.

Varma, A. H., Ricles, J. M., Sause, R. & Lu, L.-W. 2002. Seismic behavior and modeling of high strength composite concrete-filled steel tube (CFT) beam-columns. J. of Construct. Steel Research, 58, pp.725-758.